Climate induced Congestion in Ports: General Equilibrium Consequences on Transportation and Trade

Jeanne Astier*

January 2026

Preliminary and Incomplete.
Please do not circulate.

Abstract

This paper studies the impact of climate change on ports and its consequences for maritime transportation and international trade. Rising sea levels and associated weather events threaten port operations in a spatially heterogeneous way. Because container shipping operates as a global network, local disruptions propagate, creating spillovers that also affect ports not directly exposed. I combine high-frequency data on shipping and marine weather to estimate how adverse conditions reduce port efficiency and raise transportation costs. I embed these estimates in a trade model with networked shipping and endogenous port congestion, allowing me to compute counterfactuals. Using climate projections of sea-level rise, I quantify the welfare effects of increasing maritime transportation costs. By 2100, ports are projected to experience water-level increases of up to 1.3 meter, leading to losses of up to 1.1% in real output. A port's welfare loss arises not only from its own exposure to rising water levels (direct effect), but also from spillovers generated by sea-level rise at other ports (indirect effect). As a result, I show that even ports facing no local increase in water levels will suffer welfare losses due to global sea level rise.

Keywords: shipping, climate change, trade, weather, transportation, sea level rise

*Center for Research in Economics and Statistics (CREST), Institut Polytechnique de Paris. Email: jeanne.astier@ensae.fr.

1 Introduction

The impact of climate change on economic outcomes has been widely documented, in particular for weather events happening on land through the channels of agriculture, productivity, capital. The role of trade in mitigating climate change impact is also extensively studied by the environmental economics literature (Costinot et al., 2016; Gouel & Laborde, 2021; Carleton et al., 2023). However, the sensitivity of trade itself to climate change seems overlooked: trade costs might be impacted by climate change. This could happen through the channel transportation, which can be impacted by weather conditions both on land and at sea. Looking at the effect of climate change on trade costs allows to uncover a new part of the climate damage function, and to provide new elements on the debate of trade as a mitigation factor.

Transportation is indeed essential for trade, and very sensitive to weather conditions – especially maritime transport. International trade is heavily relying on maritime freight: about 80% of traded goods are seaborne (UNCTAD, 2023). Yet, the shipping sector is often disrupted by weather events, especially those affecting port infrastructures.[1] Climate change is expected to worsen the weather conditions affecting ports, through sea-level rise and associated weather events (wind, waves, storm surge, coastal flooding...) (Pörtner et al., 2019). Such adverse weather translates into non-operability days for the ports, during which their activity is stopped or significantly reduced (Izaguirre et al., 2021). Their reduced capacity to receive ships might in turn cause congestion, resulting in increases of transportation costs (Brancaccio et al., 2024). Given the network structure of shipping (Heiland et al., 2019; Brancaccio et al., 2020; Ganapati et al., 2021), the effect of these local weather shocks could propagate to other ports and shipping routes, triggering a ripple effect with global consequences.

This paper studies the global impact of climate change effects on ports and its consequences on international trade, in the context of the container-shipping network. I leverage detailed shipping and weather data to estimate how weather shocks affect ports efficiency, and hence raise transportation costs. I then include this effect in a model of international trade with a shipping network, featuring port congestion, based on Allen & Arkolakis (2022). This model is then used to estimate counterfactuals with sea level rise projections: I can quantify the global effects on transportation and trade given the spillover mechanisms at play, as well as the spatial distribution of the heterogeneous local effects.

I rely on satellite automatic identification system (AIS) technology, a novel source of data inscreasingly used in the trade literature (Heiland et al., 2019; Brancaccio et al., 2020; Ganapati et al., 2021). I observe the exhaustive universe of port calls made by containerships in about

[1] See for instance the closure of New York and New Jersey ports in October 2012 because of Hurricane Sandy, more recently the closure of Florida ports during hurricane Milton in October 2024.

1,700 ports between 2015 and 2023, with their exact hour and date. These data allow to build measures of port efficiency, such as the port dwell time (the time ships spend in the port to be unloaded and reloaded) or the port incoming traffic (number of entering calls). I combine these measures with weather data at the location of the ports: wave height and water level daily averages from the global reanalysis ERA-5 dataset (Hersbach et al., 2023). Reduced-form evidence shows that wave height and water level significantly affect port efficiency: a jump from the 25th to the 75th percentile of daily average wave height increases the dwell time by 2.5% and reduces the entering traffic by 7.9%. I find that this effect is non-linear and mostly driven by days with extreme wave height. The results also highlight spillovers: I construct port linkages using the shipping data, and find that a port's efficiency is affected not only by its own local weather, but also by weather in upstream and downstream ports.

To understand more precisely the spillover mechanisms and quantify global effects of weather shocks, I rely on a spatial economic model with optimal shipping route choice and endogenous traffic costs. I adapt the workhorse model of Allen & Arkolakis (2022), often used to study transportation between cities (e.g. Fuchs & Wong 2024), to an international trade and shipping setting. I consider that firms can export the goods they produce through ports, that are connected by a shipping network. To export from an origin to a destination, firms choose an optimal route that can go through several intermediate ports.[2] As opposed to the road network considered by Allen & Arkolakis (2022), I model congestion not on the *links* of the network but on the *nodes* – i.e. the ports: the cost of going through a port depends on the congestion in this port. Indeed, Brancaccio et al. (2024) show that a greater number of ships in a port forces ships to queue and hence increases the ships dwell time and service cost. I further assume that congestion in a port depends not only on the traffic if faces but also on the availability of its infrastructures, that can be affected by weather shocks. Using exact hat algebra techniques, I can then solve the model to determine the welfare effects of a counterfactual weather.

To quantify counterfactual scenarios, I need to estimate two key parameters: the elasticities of ships' dwell time to port congestion and to weather shocks. I leverage detailed AIS shipping data to estimate those, relying on a specification derived from the model – similarly to Fuchs & Wong (2024) but with an additional weather effect. The estimates I obtain show that a 1% increase in port traffic raises ships dwell time by 0.25%, while +1m water level increases the dwell time by 1.4% – effects significant at the 5% level with a strong first stage.

Using these estimates and taking other structural parameters' values from the literature, I run a fixed point algorithm to solve for counterfactuals. I rely on country-level population and economic outcome from the World Penn Tables, and allocate those to ports by creating port

[2] Ganapati et al. (2021) highlight that most of shipping transportation is indirect, the goods stopping in several intermediate ports between the origin and destination ports.

catchment areas. I rely on IPCC's sea level rise projections (Garner et al., 2022) to compute the change in water level for each port: there is significant heterogeneity, with some ports facing little to no increase in water level while other will experience more than +1m by 2100 (according to scenario SSP5-8.5). The model predicts a significant welfare loss, up to -1.1% of real outcome for the most affected ports (in the Philippines, East Coast of the USA).

The counterfactual exercise results show that a port's welfare loss is correlated with its own rise in water level, but not perfectly. Indeed, even the ports facing no change is water level will suffer a decrease of real outcome. This result highlight the importance of indirect effects coming from other ports through the shipping network.

This project builds on the trade literature including transportation network. While this literature originally considers land transportation infrastructures at the country level, like highways or railroads (Fajgelbaum & Schaal, 2020; Allen & Arkolakis, 2022; Fuchs & Wong, 2024), an increasing body of works adapts these tools to study maritime transportation (Heiland et al., 2019; Brancaccio et al., 2020; Ganapati et al., 2021; Ludwig, 2024). I contribute to this literature by modeling further the specificities of the shipping network – in particular, displacing congestion from to *links* of the network to the *nodes*, based on the framework of Allen & Arkolakis (2022). This project also aims at studying transportation in an international context, rather than between cities of a same country: I further adapt the workorse model of Allen & Arkolakis (2014) to include specificities of international trade such as labor immobility and trade deficits between regions. I face the issue of non-isomorphism between the trading entities (countries) and transportation nodes (ports). While other papers in an international context consider only the country level, aggregating ports (Ganapati et al., 2021; Ludwig, 2024)[3], I try to provide a mapping between countries and ports by building port catchment areas.

I also relate to the growing literature studying shipping from satellite AIS data. Most of this literature focuses on ships trips in a trade context (Heiland et al., 2019; Brancaccio et al., 2020; Ganapati et al., 2021), while a recent paper by Brancaccio et al. (2024) uses these data to study ports at the micro, country level. I try to connect these two approaches by including port congestion mechanisms identified by Brancaccio et al. (2024) in a global trade setting. The closest paper related to my work is Fuchs & Wong (2024), which studies a multi-modal transportation network including, among others, nodes congestion, also estimated using AIS data. My contribution with regard to this paper is to go from a country-level approach to a global setting and to propose a novel instrument for the estimation of congestion elasticity. I also propose to study a new mechanism which, to the best of my knowledge, has not been studied yet in this trade and shipping literature: the effect of weather shocks.

[3]Which results in disregarding land-locked countries.

This weather shocks mechanism relates the paper to the environmental literature, first on the strand trying to quantifying the effect of climate change on economic outcomes. This impact has been widely documented for weather events happening on land – such as temperature shocks (Dell et al., 2012), hurricanes (Deryugina et al., 2018), floodings (Balboni et al., 2023), wildfires (Wang et al., 2021) ... – through channels like agriculture, productivity, capital. I propose to study sea weather shocks, focusing on wave height, and to uncover a new channel, the transportation sector. While some environmental works have been investigating the link between transportation and climate change, they mostly focus on how transportation contributes to climate change through emissions (see for instance Ludwig 2024 for the shipping sector). My perspective is rather to study how climate change related weather events can impact the transportation sector.

Finally, I also build on works studying in a reduced-form way the local impact of weather shocks on port operations (Becker et al., 2018; Christodoulou et al., 2019). I try to include these local effects in a global shipping framework, to include spillovers and quantify a global impact on economic outcome. I rely on the work of climate scientists Izaguirre et al. (2021) which provide evidence of the sea weather shocks affecting port operations and document the spatially heterogeneous effects that climate change will have on ports.

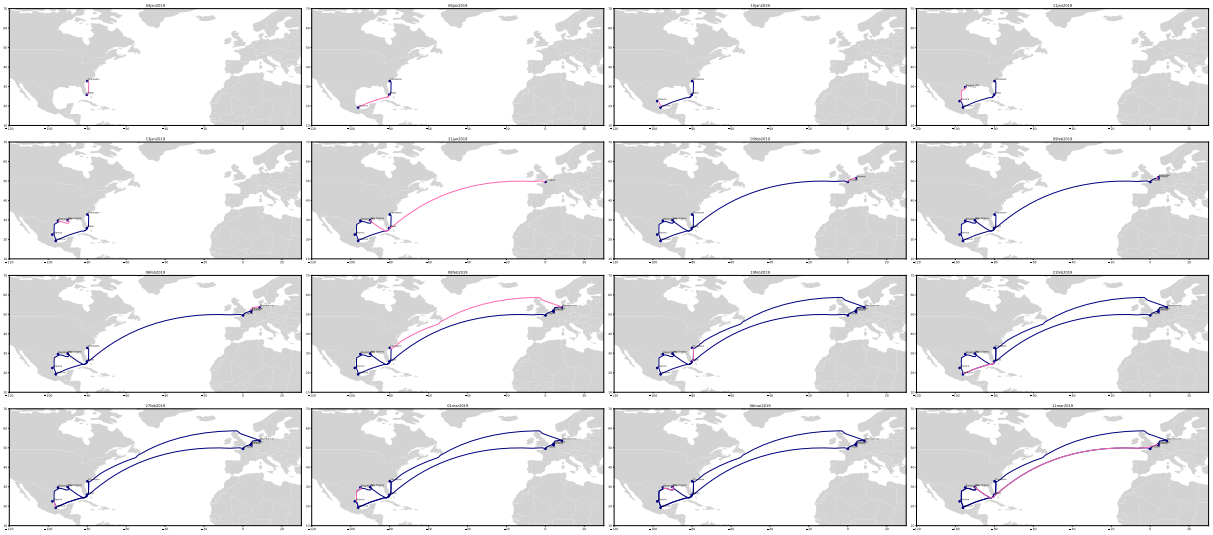
The rest of the paper is organized as follows. Section 2 gives some elements of context about container-shipping. Section 3 presents the data used and provides reduced-form evidence of the effect of weather shocks on port efficiency. Section 4 details the economic geography model with shipping. I estimate the key parameters of this model in section 5. Section 6 presents the counterfactual exercises and their results. Finally, section 7 presents current work in progress about network flexibility.

2 Context about Container-Shipping

Containerships carry essentially manufactured goods. As explained by Brancaccio et al. (2020), they operate like a public bus system, with a pre-specified set of ports (called a *service*) at which a ship stops successively. At each port, containers can enter or leave the ship. They can also change ship (trans-shipment). Figure 1 shows an example of containership service between Europe and America, going through the ports of Charleston - Miami - Veracruz - Altamira - Bayport - New Orleans - Le Havre - Antwerp - Rotterdam - Bremerhaven.

The set of services constitutes the containership *network structure*: this is the set of all the direct links between two ports that exist, i.e. the set of links over which containers can flow.

Figure 1: Example of a containership service between America and Europe



Note: these maps represent the trajectory of a containership from January to March 2019. Each pink line depicts the journey of the ship made on the day shown at the top of each map; the dark blue lines depict the journeys made by the ship in the previous days. The first row first column map shows the first trip of the ship from Charleston to Miami on January 4th; the first row second column map shows the next trip from Miami to Veracruz on January 6th; then from Veracruz to Altamira, etc. On Februry 8th (third row second column), the ship ends its service by going back to Charleston. It then starts another round, going through the same ports.

This network is sparse: not all pairs of ports are directly connected. As a consequence, containers traveling from an origin to a destination might go through several intermediate ports, just because these ports are part of the ship service. For instance, in the service depicted in Figure 1, if a firm wants to export a container from New Orleans to Rotterdam, it would be stopping at Le Havre and Antwerp in between. In this sense, most of container-shipping is indirect (Ganapati et al., 2021). This is quite different from bulk carriers from instance, that would go directly from origin to destination without intermediate stops – operating like a taxi, rather than a bus. This indirect structure of shipping creates a potential for spillover effects: a port being down won't only affect the goods having this port as an origin or a destination, but also all the goods flowing through this port as an intermediate stop. For instance in Figure 1, containers going from New Orleans to Rotterdam would be impact by a disruption at Antwerp.

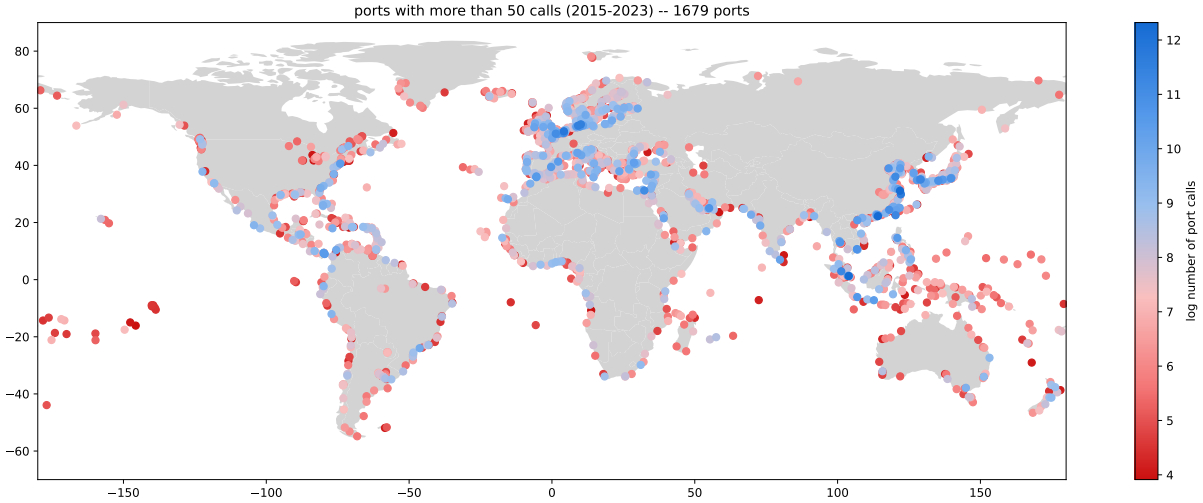
In the work presented below, I consider the network structure as fixed and study how traffic flows reallocate within this structure. However, the network structure itself might evolve, with links being created or deleted. Exploring the evolution of the network structure is work in progress, presented in Section 7.

3 Data and Reduced-Form Evidence

3.1 Shipping and Weather Data

AIS shipping data I use shipping data based on satellite automatic identification system (AIS) technology, provided by Alphaliner. The dataset covers all containerships and their detailed port calls (i.e. anytime they enter or leave a port, with the exact position and time) between 2015 and 2023. I observe a large set of ports (around 1,700) all around the world, with varying traffic intensity, as the Figure 2 shows.

Figure 2: Ports observed in the shipping data, by traffic intensity (2015-2023)



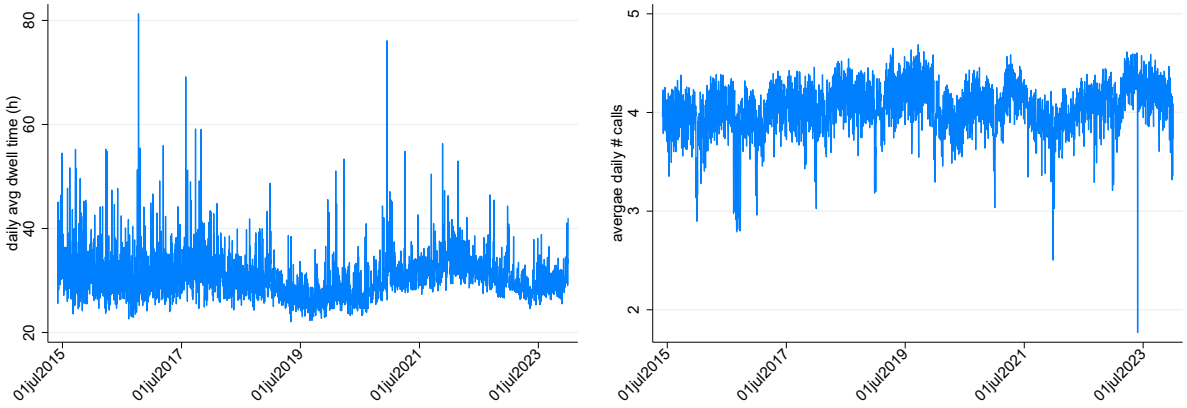
Note: The traffic intensity is computed as the logarithm of number of entering port calls over the total period.

For each port, I can use AIS shipping data to build two measures of port efficiency (Brancaccio et al., 2024). The port dwell time measures how long ships spend in the port (I compute it as their time of departure − time of arrival). It describes the time required by the port to unload and reload the ships, and hence measures the efficiency of port operations. The number of entering port calls measures the port traffic and its attractiveness. Figure 3 show descriptives of these two measures at the weekly frequency for the top 400 ports (in terms of traffic over the 2015-2023 period).[4] It highlights the significant volatility in port efficiency.

Sea weather data Port efficiency can be affected by various weather factors (Izaguirre et al., 2021). I consider four weather measures impacting ports: significant wave height, wind speed, total precipitation, total water level (in deviation from 1986-2005 average). I collect daily values for these four variables from the global reanalysis ERA-5 dataset (Hersbach et al., 2023). I combine these gridded data at the 0.25°x 0.25° level with ports geographical positions, to get daily

[4]These ports will be the ones considered for counterfactuals later on.

Figure 3: Measures of efficiency for the top 400 ports in the shipping data (2015-2023)



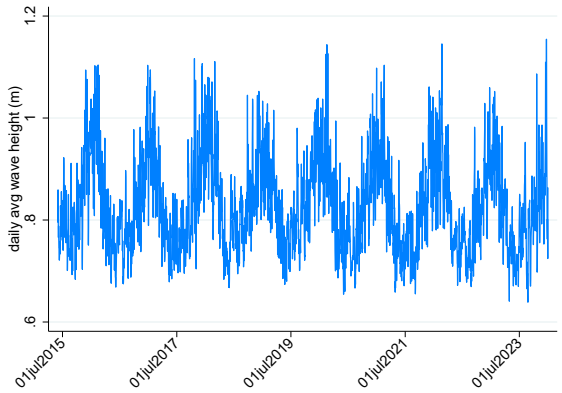
(a) Dwell time

(b) Number of entering calls

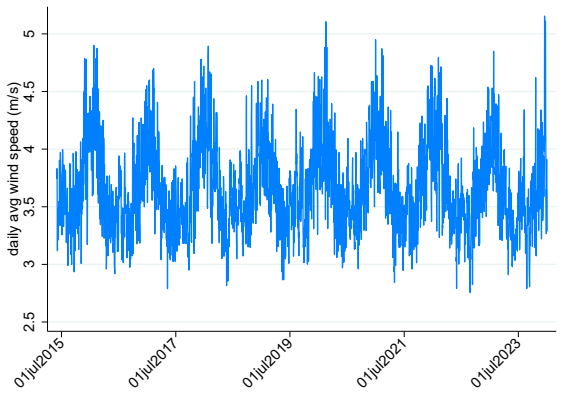
observations of port weather. Figure 4 shows the evolution of the four weather variables over the period for the top 400 ports (in terms of traffic over the 2015-2023 period). Wave height and wind speed time series display a clear seasonality, with higher values around December and lower values around June. The periodicity is also observed but less salient for precipitation, and even less for total water lever. For all 4 variables, there is significant volatility between days – this is what will be exploited for the reduced-form evidence exercise.

The correlation of these different weather measures is displayed in Figure B.1. Wave height is positively correlated with wind speed, as well as with precipitation (to a lesser extent). Water level however is not correlated with any other weather measure. I will hence focus on wave height and water level for the reduced-form evidence presented below.

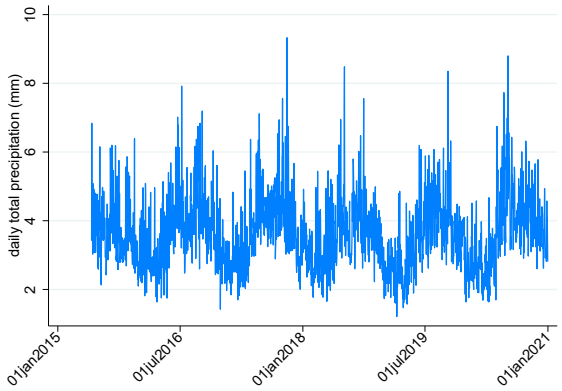
Figure 4: Average daily weather measures in the top 400 ports in the shipping data (2015-2023)



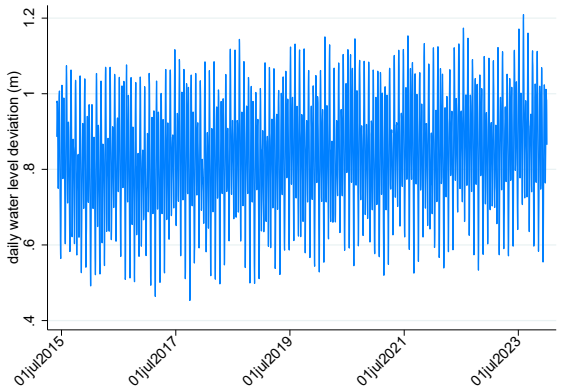
(a) wave height



(b) wind speed



(c) precipitation



(d) total water level

3.2 Reduced-Form Evidence: Effect of Weather Shocks on Port Efficiency

I combine shipping data with wave height and water level observations, to produce evidence of weather impact on port efficiency. I first provide evidence of the direct effect of a port's own local weather shocks on its efficiency, then highlight spillover mechanisms between the different ports connected through the shipping network.

3.2.1 Direct effect of local shocks

I test the effect of a port's weather on its efficiency with the following specification:

$$y_{it} = \alpha + \beta \text{ weather}_{it} + \delta_i + \delta_t + \epsilon_{it} \tag{1}$$

where y_{it} is a measure of port i efficiency during day t (log average dwell time or total number of entering calls), weather_{it} is the weather at port i during day t (average significant wave height or maximum total water level). δ_i is a port fixed-effect, δ_t a day fixed effect; in alternative specifications, I include other fixed-effects such as port-month or country-day. When y_{it} is the number of port calls, I estimate a Poisson model. Standard errors are clustered at the port or at the country level.

Wave height Results in Table 1 show a significant effect of daily wave height on port efficiency: +1m of wave height (which is equal to around 1.5 standard deviation) increases the dwell time by 2 to 3% and reduces the number of entering calls by 10 to 11%. These effects are robust across the different sets of fixed effects included and level of clusterisation of the standard errors.

Table 1: Effect of wave height average on port efficiency (daily)

	(1)	(2)	(3)	(4)
	log time	# calls	log time	# calls
wave height	0.0329***	-0.1010***	0.0207***	-0.1160***
	(0.0028)	(0.0051)	(0.0042)	(0.0150)
date (day) FE	✓	✓		
port FE	✓	✓		
port-month FE			✓	✓
country-day FE			✓	✓
SE cluster level	port	port	country	country
# observations	2,024,358	5,223,035	1,818,063	4,134,985
# clusters	1,679	1,679	128	132

Standard errors in parentheses

* $p < 0.10$, ** $p < 0.05$, *** $p < 0.01$

Instead of accounting linearly for daily wave height, I can consider bins of daily wave height to

capture potential non-linear effects. Izaguirre et al. (2021) define an *absolute* wave height threshold above which ports cannot operate at all, at 2.5m. Since I also want to capture when port operations are only partially disrupted, I consider a slightly lower threshold, 2m (corresponding roughly to the 95th percentile of daily wave height observations across ports, see Figure B.2). However, the effect of a same wave height might be different across ports depending on how often they face it, their infrastructure, etc. To account for this, I also consider a *relative* wave height threshold corresponding to the 95th percentile of wave height for each port over the period (2015-2023). Results in Table 2 show consistent magnitudes: when daily wave height exceeds either the absolute or the relative threshold, dwell time in the port increases and incoming traffic decreases. The effect of local weather shocks on a ports' efficiency thus seems to be driven by extreme events.

Table 2: Non-linear effect of waves height on port efficiency (daily)

	(1) log time	(2) # calls	(3) log time	(4) # calls	(5) log time	(6) # calls	(7) log time	(8) # calls
wave height >2m	0.0467***	-0.1643***	0.0251***	-0.1365***				
	(0.0055)	(0.0123)	(0.0075)	(0.0213)				
wave height > p95					0.0342***	-0.1835***	0.0218***	-0.1536***
					(0.0043)	(0.0102)	(0.0055)	(0.0301)
date (day) FE	✓	✓			✓	✓		
port FE	✓	✓			✓	✓		
port-month FE			✓	✓			✓	✓
country-day FE			✓	✓			✓	✓
SE cluster level	port	port	country	country	port	port	country	country
# observations	2,024,358	5,223,035	1,818,063	4,134,985	2,024,358	5,223,035	1,818,063	4,134,985
# clusters	1,679	1,679	128	132	1,679	1,679	128	132

Standard errors in parentheses

* $p < 0.10$, ** $p < 0.05$, *** $p < 0.01$

Total water level Similarly, Table 3 shows a significant effect of daily total water level on port efficiency: +1m of total water level compared to 1986-2005 average (which is equal to around 1.2 standard deviation) increases the dwell time by 1 to 2% and reduces the number of entering calls by 2 to 3%. Results in Table 4 show significant impact for the *relative* threshold mostly. Overall, water level effects on port efficiency have a lower magnitude than wave height effects (Tables 1 and 2); however they are still important to take into account as water level is the main factor that will evolve with climate change and sea level rise.

Additional results Results for other weather variables (wind speed, total precipitation) are presented in appendix C.1, and display a similar pattern: higher levels of wind speed and precipitation are associated to an increase in port dwell time and a decrease in incoming traffic.

Table 3: Effect of total water level on port efficiency (daily)

	(1) log time	(2) # calls	(3) log time	(4) # calls
water level	0.0212***	-0.0253***	0.0137***	-0.0257**
	(0.0033)	(0.0051)	(0.0035)	(0.0119)
date (day) FE	✓	✓		
port FE	✓	✓		
port-month FE			✓	✓
country-day FE			✓	✓
SE cluster level	port	port	country	country
# observations	2,034,605	5,265,178	1,818,063	4,134,985
# clusters	1,679	1,679	128	132

Standard errors in parentheses

* $p < 0.10$, ** $p < 0.05$, *** $p < 0.01$

Table 4: Non-linear effect of total water level on port efficiency (daily)

	(1) log time	(2) # calls	(3) log time	(4) # calls	(5) log time	(6) # calls	(7) log time	(8) # calls
water level >2m	0.0032	-0.0166***	-0.0005	-0.0130**				
	(0.0050)	(0.0045)	(0.0036)	(0.0056)				
water level >p95					0.0274***	-0.0400***	0.0138***	-0.0266**
					(0.0037)	(0.0048)	(0.0045)	(0.0104)
date (day) FE	✓	✓			✓	✓		
port FE	✓	✓			✓	✓		
port-month FE			✓	✓			✓	✓
country-day FE			✓	✓			✓	✓
SE cluster level	port	port	country	country	port	port	country	country
# observations	2,034,605	5,265,178	1,818,063	4,134,985	2,034,605	5,265,178	1,818,063	4,134,985
# clusters	1,679	1,679	128	132	1,679	1,679	128	132

Standard errors in parentheses

* $p < 0.10$, ** $p < 0.05$, *** $p < 0.01$

I also consider additional specifications to enrich the results. In appendix C.2, I show in an event-study setting that weather shocks also have an effect before and after the exact moment they actually happen. Port efficiency is indeed reduced not only on the day when it experiences extreme weather, but also during the days before and after, as illustrated with wave height. This suggests that the daily effects observed above might only been a lower bound of the total weather effect.

Appendix C.3 performs similar reduced-form exercises but at the *ship* level, rather than aggregating by port. The results are consistent, a higher wave height in a port increasing the dwell time of all ships entering into this port. Specifications at the port level are preferred because they allow to observe two measures efficiency: (average) dwell ship time and port traffic. At the ship level, one might only look at dwell time and hence only observe the intensive margin of weather of port efficiency (how long ships spend in the port), not the extensive margin (whether ships actually go into the port).

In appendix C.4, I additionally show that weather *inside* a port might have an effect on ships behavior *outside* of ports: when a port is disrupted, ships might prefer to wait outside of the port (to avoid paying additional port fees). I indeed find that high wave height in origin or departure port increase the trip duration of ships. This suggests once again that the effects observed in the ports might be only a lower bound of the full effects, since they do not capture ships waiting outside of ports.

An important consideration is why weather conditions in ports warrant greater analytical emphasis than those encountered at sea during the transit between ports. While it is true that vessels typically spend a larger share of their voyage at sea – where they may be exposed to adverse phenomena such as storms, high waves, and strong winds – maritime navigation allows for considerable flexibility. In particular, vessels can adjust their course in response to meteorological forecasts, a practice commonly referred to as weather routing. In contrast, ports are geographically fixed and thus more vulnerable to local weather disruptions. In addition, the adverse effects of weather shocks in ports are amplified by infrastructure constraints leading to congestion, while the open sea is unconstrained by physical infrastructure. To empirically assess the differential importance of weather conditions in ports versus those along the maritime route, I conduct a comparative analysis of their effects on shipping duration in Appendix C.5. The results indicate that adverse weather in ports has a more pronounced effect on shipping times, as it influences both port dwell times and the duration of journeys between ports.

3.2.2 Spillover effects

Because the ports are connected through a shipping network (Heiland et al., 2019; Brancaccio et al., 2020; Ganapati et al., 2021), the efficiency of a port might be affected not only by its own weather but also by the weather of upstream and downstream ports. The network connecting ports can be observed in the shipping data: for a given ship s stopping in a port i on day t, one might also retrieve the previous port $i-1$ the ship s stopped at, as well as the one before and so on ($i-2$, $i-3$, etc.). These are the upstream ports. Similarly, one might also observe the downstream ports, where the ship s is going afterwards ($i+1$, $i+2$, etc.). To test for spillovers along the shipping network, I test if the efficiency of port i is impacted by weather shocks in upstream and downstream ports:

$$\ln(\text{time}_{sit}) = \sum_{h=0}^{4} \beta_h^U \text{ weather}_{i-h,t} + \beta \text{ weather}_{i,t} + \sum_{h=0}^{4} \beta_h^D \text{ weather}_{i+h,t} + \delta_{si} + \delta_t + \delta_{iy} + \epsilon_{sit} \quad (2)$$

where time_{sit} is the time spent by ship s in port i on day t, $\text{weather}_{i,t}$ is the weather in port i on day t, $\text{weather}_{i-h,t}$ is the weather in upstream port $i-h$ and $\text{weather}_{i+h,t}$ is the weather in downstream port $i+h$.[5] δ_{si} is a ship-port fixed-effect, δ_t a date fixed-effect and δ_{iy} a port-year fixed-effect.

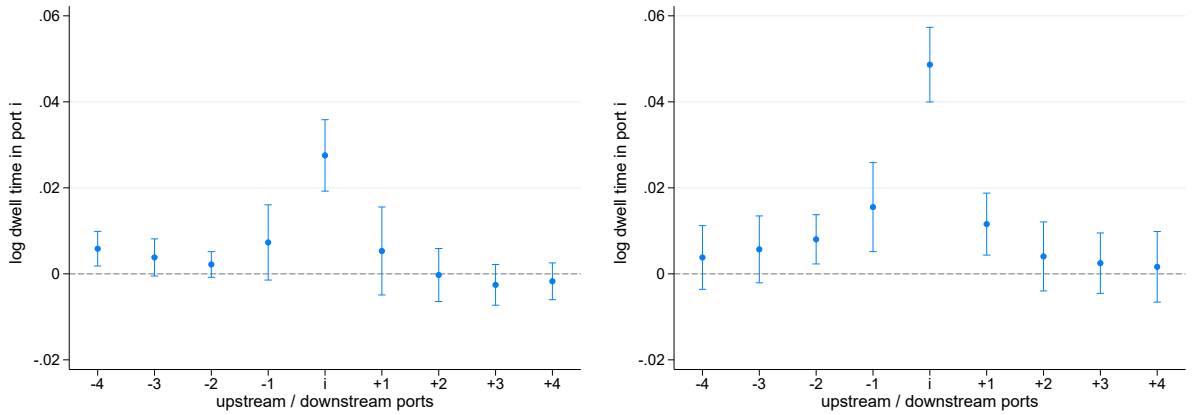
The estimated coefficients for weather measured as wave height[6] are depicted in Figure 5. As already shown above, port efficiency is affected by its own local weather: a daily wave height greater than 2m is associated with a 5% increase in port dwell time, compared to a day with wave height below 2m (right panel, coefficient i). Weather shocks in upstream and downstream ports also seem to play a role on port i's efficiency: a daily wave height greater than 2m in port $i-1$ or $i+1$ is associated with a 1.7% increase in port dwell time in i. Wave height in up and downs-tream ports has effects of the same sign as the local wave height, though of a lower magnitude. These effects are attenuating as the we move away from port i along the shipping network.

The mechanisms explaining these results could come from congestion propagation: when a port is affected by local bad weather, it cannot service ships and get congested. Ships then arrive late at the next port, which disrupts its schedule, creating congestion there even in the absence of local weather shock. These findings point toward the importance of weather shocks spillovers through the shipping network.

[5] Note that I consider weather at all ports on the same day t. For alternative specifications introducing lags for upstream ports and lead for downstream ports, see appendix C.6.

[6] When measuring weather as total water level, there is not enough variability bewteen places to retrieve significant coefficients.

Figure 5: Effect of upstream, local, and downstream wave height on port efficiency



(a) average wave height

(b) wave height >2m

4 Economic Geography Model with Shipping

The reduced-form evidence shows that port efficiency is affected by weather shocks, and that these effects propagate through the shipping network. To understand better the spillovers mechanism and estimate the global effect of weather shocks, I use an economic geography model of trade with shipping. I rely on the workhorse model of Allen & Arkolakis (2022) (A&A henceforth), designed to study road or rail transportation between cities, and adapt it to an international trade and shipping setting. I present the model below, highlighting the differences from A&A. In the presentation of the model, I abstract from time subscripts t for clarity, but I consider that this static model can be repeated over time.

4.1 Model set up

Consider a finite number of countries $c \in \{1, ..., C\} \equiv \mathcal{C}$, inhabited by $\bar{L}$ individuals, and a finite number of ports $i \in \{1, ..., N\} \equiv \mathcal{N}$ $(N > C)$.[7] The ports are located in countries – countries can have between zero and several ports. The countries are populated by individuals (resp. firms), who can locate in different regions of the country; they are related to the closest port of their region from which they can import and consume (resp. produce and export) goods. Each port thus has a catchment area where are located individuals and firms related to this port. Let $\omega_{c,i}$ denote the share of individuals and firms of country c that belong to port i catchment area.

Ports $i \in \mathcal{N}$ are connected by a transportation (shipping) network, represented by two matrices:

[7] In the original A&A model, there is an isomorphism between regions c and transport nodes i are they consider cities. Here, I introduce the distinction between the two as I am considering trade between countries but transportation between ports.

- as in A&A, a $N \times N$ matrix of links costs $\mathbf{T} = [t_{kl} \geq 1]$, where t_{kl} is the ad valorem (iceberg) cost incurred from moving directly from $k \in \mathcal{N}$ to $l \in \mathcal{N}$ along a link (if there is no link, then $t_{kl} = +\infty$).
- an additional $N \times 1$ matrix of nodes costs $\mathbf{P} = [p_k \geq 1]$, where p_k is the ad valorem cost incurred from going through port $k \in \mathcal{N}$.

Goods move from an origin port i to a destination port j through a route r, defined as a sequence of links and intermediate nodes connecting i to j. A route of length K from i to j is a sequence of $K+1$ locations and the links in between: $r \equiv \{r_0 = i, r_1, ..., r_K = j\}$. Since iceberg costs are multiplicative, the total cost of route r is

$$p_i \times t_{i,k_1} \times p_{k_1} \times t_{k_1,k_2} \times ... \times t_{k_{K-1},j} \times p_j = \underbrace{\left(\prod_{l=0}^{K} p_{r_l}\right)}_{\text{cost of nodes}} \underbrace{\left(\prod_{l=1}^{K} t_{r_{l-1},r_l}\right)}_{\text{cost of links}} \tag{3}$$

There are multiple routes going from origin i to destination j: let $\mathcal{R}_{ij}$ denote their set.

Goods are traded across port catchment areas (also referred to as locations). In this international setting, labor is considered to be immobile between locations.[8] Each individual related to port catchment area $i \in \mathcal{N}$ supplies one unit of labor inelastically (labor being the only factor of production) for a wage w_i. Individuals also purchase quantities of a continuum of goods $\nu \in [0, 1]$ with constant elasticity of substitution σ. Let Y^W denote the total income in the economy. In what follows, average per capita income is taken as the numeraire: $Y^W/\bar{L} = 1$.

Each location $i \in \mathcal{N}$ is endowed with a constant return to scale technology for producing and shipping each good $\nu \in [0, 1]$ to each destination $j \in \mathcal{N}$ along each route $r \in \mathcal{R}_{ij}$. The technology is origin-destination-route specific, subject to idiosyncratic shocks $\epsilon_{ij,r}(\nu)$ – following Eaton & Kortum (2002), $\epsilon_{ij,r}(\nu)$ is independently and identically Fréchet-distributed across routes and goods, with a scale parameter $1/\bar{A}_i$ (capturing origin-specific efficiency) and a shape parameter θ (regulating the shock dispersion).

Under perfect competition, the price in destination j of a good sourced in origin i and shippped along route r is given by

$$p_{ij,r}(\nu) = w_i \frac{\left(\prod_{l=0}^{K} p_{r_l}\right)\left(\prod_{k=1}^{K} t_{r_{k-1},r_k}\right)}{\epsilon_{ij,r}(\nu)} \tag{4}$$

Individuals in location j purchase each good $\nu \in [0, 1]$ from the cheapest source (i.e. origin-route).

[8] As opposed to A&A setting that considers cities within a country, where labor is perfectly mobile.

4.2 Gravity and equilibrium

Following closely A&A, given the Fréchet distribution of origin-destination-route specific productivities, the probability that $j \in \mathcal{N}$ purchases good $\nu \in [0,1]$ from $i \in \mathcal{N}$ along route $r \in \mathcal{R}_{ij}$ can be written as:

$$\pi_{ij,r} = \frac{\left(w_i/\bar{A}_i\right)^{-\theta}\left(\prod_{l=0}^{K} p_{r_l}^{-\theta}\right)\left(\prod_{l=1}^{K} t_{r_{l-1},r_l}^{-\theta}\right)}{\sum_{k\in\mathcal{N}}\left(w_k/A_k\right)^{-\theta}\sum_{r'\in\mathcal{R}_{kj}}\left(\prod_{l=0}^{K} p_{r'_l}^{-\theta}\right)\left(\prod_{l=1}^{K} t_{r'_{l-1},r'_l}^{-\theta}\right)} \tag{5}$$

The total value of goods shipped from i to j, X_{ij} is obtained by summing across all routes r connecting i to j. As in Eaton & Kortum (2002), the probability of purchasing a good is equal to the expenditure share, yielding

$$X_{ij} = \sum_{r\in\mathcal{R}_{ij}} \pi_{ij,r} E_j = \frac{\left(w_i/\bar{A}_i\right)^{-\theta}\tau_{ij}^{-\theta}}{\sum_{k\in\mathcal{N}}\left(w_k/\bar{A}_k\right)^{-\theta}\tau_{kj}^{-\theta}} E_j \tag{6}$$

where τ_{ij} is the transportation cost from i to j – with an additional nodes cost term compared to A&A:

$$\tau_{ij} \equiv \left(\sum_{r\in\mathcal{R}_{ij}}\left(\prod_{l=0}^{K} p_{r_l}^{-\theta}\right)\left(\prod_{l=1}^{K} t_{r_{l-1},r_l}^{-\theta}\right)\right)^{-\frac{1}{\theta}} \tag{7}$$

Market clears at the equilibrium: total income Y_i in each location is equal to its total sales, and total expenditure E_i is each location is equal to its total purchases:

$$Y_i = \sum_{j=1}^{N} X_{ij}\ , \quad E_i = \sum_{j=1}^{N} X_{ji}, \tag{8}$$

Under these conditions, one can then retrieve the usual gravity equation:

$$X_{ij} = \tau_{ij}^{-\theta} \times \frac{Y_i}{\Pi_i^{-\theta}} \times \frac{E_j}{P_j^{-\theta}} \tag{9}$$

where Π_i and P_j are the market access terms (or multilateral resistance terms) as in Anderson & Van Wincoop (2003). Π_i is a producer price index capturing the (inverse) producer market access, while P_j is the consumer price index capturing the (inverse) consumer market access terms:

$$\Pi_i \equiv \left(\sum_j \tau_{ij}^{-\theta} E_j P_j^{\theta}\right)^{-\frac{1}{\theta}}, \quad P_j \equiv \left(\sum_i \tau_{ij}^{-\theta} Y_i \Pi_i^{\theta}\right)^{-\frac{1}{\theta}} \tag{10}$$

I introduce the same notations as A&A and define $y_i \equiv Y_i/Y^W$ and $l_i \equiv L_i/\bar{L}$ as the share

of total income and total labor in location $i \in \mathcal{N}$, respectively. As opposed to A&A, labor is immobile: l_i is thus exogenously determined ($l_i = \bar{l}_i$) and there is no equalization of welfare across locations.

In this international trade setting, I assume that trade is imbalanced:[9] denoting D_i the deficit, $E_i = Y_i + D_i$ (with $\sum_i D_i = 0$). I further assume that the deficit is a share of local outcome, as in Costinot & Rodríguez-Clare (2014): $D_i = \kappa_i Y_i$. Hence

$$E_i = (1 + \kappa_i) Y_i \tag{11}$$

Combining these equations[10], I obtain the following equilibrium conditions:

$$\bar{A}_i^{-\theta} \bar{l}_i^{-\theta} y_i^{1+\theta} = \sum_j \tau_{ij}^{-\theta} (1 + \kappa_j) y_j P_j^{\theta} \tag{12}$$

$$P_i^{-\theta} = \sum_j \tau_{ji}^{-\theta} \bar{A}_j^{\theta} \bar{l}_j^{\theta} y_j^{-(\theta+1)} \tag{13}$$

Given $\{\bar{A}_i\}$, $\{\bar{l}_i\}$, $\{\tau_{ij}\}$, $\{\kappa_i\}$, 12 and 13 constitute a system of $2N$ equations can be solved to get equilibrium $\{y_i\}$ and $\{P_i\}$. However, similarly to A&A, I want to make the transportation costs endogenous, through traffic congestion, so that they also respond to the equilibrium distribution of y_i and P_i.

4.3 Endogenous transportation costs and weather

The first step is to write an analytical relationship between (i) transportation network characterized by links and nodes costs t_{ij} and p_i, and (ii) transportation costs τ_{ij}. I follow and adapt A&A procedure: starting from $\tau_{ij}^{-\theta} = \sum_{r \in \mathcal{R}_{ij}} \left(\prod_{l=0}^{K} p_{r_l}^{-\theta} \right) \left(\prod_{l=1}^{K} t_{r_{l-1}, r_l}^{-\theta} \right)$ (equation 7) and enumerating all possible routes,[11] it comes that

$$\tau_{ij}^{-\theta} = \sum_{K=0}^{+\infty} (\mathbf{D}^K)_{ij} \, p_i^{-\theta}$$

where $\mathbf{D}$ is the $N \times N$ matrix of general term $d_{ij} \equiv t_{ij}^{-\theta} p_j^{-\theta}$, and $(\mathbf{D}^K)_{ij}$ is the term of the i-th and j-th column of matrix $\mathbf{D}$ to the power K. Provided that the spectral radius of $\mathbf{D}$ is less

[9] A&A consider balanced trade between cities; however in international trade data, expenditures are not equal to income, i.e. countries operate either in surplus or in deficit in a given year.

[10] See Appendix A.1 for detailed derivation of the equilibrium conditions.

[11] See Appendix A.2 for detailed derivation of the analytical relationship between τ_{ij}, t_{ij} and p_i.

than one, the geometric sum can be expressed as:

$$\sum_{K=0}^{+\infty} \mathbf{D}^K = (\mathbf{I} - \mathbf{D})^{-1} \equiv \mathbf{C}^D$$

where $\mathbf{C}^D = \left[c_{ij}^D\right]$ is the Leontief inverse of the $\mathbf{D}$ matrix. As a result, the transportation cost from i to j can be written as a function of the transportation network:

$$\tau_{ij}^{-\theta} = c_{ij}^D \, p_i^{-\theta} \tag{14}$$

Once there is an analytical relationship between transportation network and transportation costs, the next step is to make the transportation network depend on traffic. Adapting A&A setting from *links* to *nodes*, I characterize the expected number of times in which a node k is used in trade between i and j, π_{ij}^k:

$$\pi_{ij}^k = \sum_{r \in \mathcal{R}_{ij}} \left(\frac{\pi_{ij,r}}{\sum_{r' \in \mathcal{R}_{ij}} \pi_{ij,r'}} \right) n_r^k \tag{15}$$

which can be rewritten as:[12]

$$\pi_{ij}^k = \frac{\tau_{ik}^{-\theta} \, p_k^{\theta} \, \tau_{kj}^{-\theta}}{\tau_{ij}^{\theta}} \tag{16}$$

This equation is close to Allen & Arkolakis (2022) as I can isolate a cost on the left of the node, the cost of the node, a cost on the right of the node. The third term of the equation might be confusing because of the positive exponent on p_k: this is because p_k already enters (negatively) in both τ_{ik} and τ_{kj}, so it is double counted.

Let Ξ_k be the node traffic in location k, i.e. the value of all goods going through node k (either because they have k as an origin or destination, or just because they transit through k as an intermediate node along their route):

$$\Xi_k = \sum_{i \in \mathcal{N}} \sum_{j \in \mathcal{N}} \pi_{ij}^k X_{ij} \tag{17}$$

This expression can be written as gravity equation for node traffic, with the same market access terms as a the gravity equation for trade flows 9:

$$\Xi_k = p_k^{\theta} \times P_k^{-\theta} \times \Pi_k^{-\theta} \tag{18}$$

A&A also show that similarly, link traffic Ξ_{kl} can be expressed with a gravity equation for

[12] See Appendix A.3 for detailed derivation of traffic expressions.

link traffic:

$$\pi_{ij}^{kl} = \frac{\tau_{ik}^{-\theta}\, t_{kl}^{-\theta}\, \tau_{lj}^{-\theta}}{\tau_{ij}^{\theta}} \tag{19}$$

$$\Xi_{kl} = t_{kl}^{-\theta} \times P_k^{-\theta} \times \Pi_l^{-\theta} \tag{20}$$

With (i) the analytical relationship between transportation cost τ_{ij} and network costs t_{ij}, p_i given by 14, and (ii) expressions of traffic given by 18 and 20, I can now introduce congestion by making the network costs t_{ij}, p_i depend on traffic – which will ultimately impact transportation cost τ_{ij}. Differently from A&A, to better represent shipping transportation (while they focus on railroads or highway transportation) I do not introduce traffic congestion on the *links* but rather on the *nodes* of the transportation network. I assume that the direct cost of traveling over a link is exogenously given (for instance by the distance of the link):

$$t_{kl} = \bar{t}_{kl} \tag{21}$$

The cost of traveling through a node will however depend in this node's traffic. More precisely, I follow Brancaccio et al. (2024) in assuming that the cost of going through a port depends on the amount of time spent on this port:[13]

$$p_k = (\text{time}_k)^{\delta_0} \tag{22}$$

where time_k is the dwell time at port k and δ_0 is the time elasticity of the transportation cost. The time spent in a port depends in turn on the port's capacity and traffic:[14]

$$\text{time}_k = \omega_k \left(\frac{\Xi_k}{K_k}\right)^{\delta_1} \tag{23}$$

where ω_k is the productivity of port k (capturing for instance the labor force, productivity shocks...) and K_k the port capacity (number of ships that can be handled simultaneously, e.g. related to the number of berths). δ_1 is the congestion elasticity of time spent at port. Finally, the port capacity is affected by weather conditions – but the effect of weather on port capacity

[13] Brancaccio et al. (2024) show that the cost for a ship to stop in a port has a fixed amount (for port services) and an additional amount depending on the time spent in the port. Their descriptive statistics show that the time-depending part constitutes the majority of the total cost. They also notice that their estimate of time cost might be a lower bound as it only includes the cost of staying in the port, but not delays for the next transportation step nor the inventory costs that importers and exporters face. Relying on this, I neglect the fixed part of port cost to focus only on the time-depending part. Additionally, Brancaccio et al. (2024) show evidence of a convex relationship between time at port and traffic, which justifies the functional form in equation 22.

[14] This functional form is a simplification compared to Brancaccio et al. (2024) who assume that time $= T\left(1 + \mathbb{1}\{Q > K\}\frac{Q-K+1}{K}\right)$ where T the service time (depending on productivity of the port, labor, number of cranes...), Q the number of ships queuing, K the port capacity. In equation 23 I abstract from the distinction between the time ships spend queuing and being unloaded/reloaded.

is heterogeneous:

$$K_k = \exp(\gamma_k \text{ weather}_k)\ \delta_k \tag{24}$$

where weather_k is a measure of weather at port k and δ_k captures other components of port capacity. γ_k captures the effect of weather on port k: this effect is port specific, as reduced-form evidence has shown that it can be heterogeneous. I follow Carleton et al. (2022) and assume that γ_k can depend on factors governing adaptation, in particular climate:

$$\gamma_k = \gamma^0 + \gamma^1 \text{ climate}_k \tag{25}$$

Combining equations 22, 23 and 24 yields

$$p_k = \omega_k^{\delta_0} \delta_k^{-\delta_0\delta_1} \exp(-\gamma_k\delta_0\delta_1 \text{ weather}_k)(\Xi_k)^{\delta_0\delta_1} \quad \text{i.e.} \quad p_k = \bar{\Gamma}_k \exp(\mu_k \text{ weather}_k)(\Xi_k)^{\lambda} \tag{26}$$

$\bar{\boldsymbol{T}} = [\bar{t}_{kl}]$ and $\bar{\boldsymbol{\Gamma}} = \left[\bar{\Gamma}_k\right]$ describe the infrastructure network, exogenously given. $\lambda = \delta_0\delta_1 > 0$ is the congestion elasticity, $\mu_k = -\gamma_k\delta_0\delta_1 > 0$ is the weather elasticity. Equation 26 is similar to the endogenous link cost equation of A&A: the transportation cost endogenously depends on traffic – the key difference in my setting being that the congestion elasticity λ plays a role on the *nodes* cost (rather than the *links*). Fuchs & Wong (2024) also include node congestion in their model, in a similar fashion. The additional weather elasticity μ is a novelty compared to both Allen & Arkolakis (2022) and Fuchs & Wong (2024).

Combining equation 26 with the gravity equation for node traffic 18 yields

$$p_k = \bar{\Gamma}_k^{\frac{1}{1-\lambda\theta}}\ e^{\frac{\mu_k}{1-\lambda\theta}\ \text{weather}_k}\ P_k^{\frac{-\lambda\theta}{1-\lambda\theta}}\ \Pi_k^{\frac{-\lambda\theta}{1-\lambda\theta}} \tag{27}$$

4.4 General equilibrium and exact hat algebra

Combining the equilibrium expressions 12 and 13 with equations 14, 20 and 27 allows to write the general equilibrium of the model with endogenous port costs.[15] Given a local geography $\{\bar{A}_i, \bar{l}_i\}_{i\in\mathcal{N}}$, an aggregate labor endowment $\bar{L}$, trade deficits $\{\kappa_i\}_{i\in\mathcal{N}}$, an infrastructure network $\bar{\mathbf{T}} = [\bar{t}_{kl}]$ and $\bar{\boldsymbol{\Gamma}} = [\bar{\Gamma}_k]$, a weather measure $\{\text{weather}_i\}_{i\in\mathcal{N}}$ and model parameters $\{\theta, \lambda, \mu_i\}_{i\in\mathcal{N}}$, the equilibrium is a distribution of economic activity $\{y_i, P_i\}_{i\in\mathcal{N}}$ satisfying:

$$\begin{aligned} y_i^{\theta+1+\frac{\lambda\theta(\theta+1)}{1-\lambda\theta}} P_i^{-\frac{\lambda\theta^2}{1-\lambda\theta}} =& \bar{L}^{-\frac{\lambda\theta}{1-\lambda\theta}} \bar{A}_i^{\frac{\lambda\theta^2}{1-\lambda\theta}+\theta} \bar{\Gamma}_i^{\frac{-\theta}{1-\lambda\theta}} e^{\frac{-\mu_i\theta}{1-\lambda\theta}\text{weather}_i} \bar{l}_i^{\frac{\lambda\theta^2}{1-\lambda\theta}+\theta} (1+\kappa_i) y_i P_i^{\theta} \\ &+ \bar{L}^{-\frac{\lambda\theta}{1-\lambda\theta}} \sum_{j=1}^{N} \bar{A}_i^{\frac{\lambda\theta^2}{1-\lambda\theta}+\theta} \bar{A}_j \bar{t}_{ij}^{-\theta} \bar{\Gamma}_i^{\frac{-\theta}{1-\lambda\theta}} e^{\frac{-\mu_i\theta}{1-\lambda\theta}\text{weather}_i} \bar{l}_i^{\frac{\lambda\theta^2}{1-\lambda\theta}+\theta} \bar{l}_j^{-\theta} y_j^{1+\theta} \end{aligned} \tag{28}$$

[15] See Appendix A.5 for detailed derivation of the equilibrium equations.

$$
\begin{aligned}
y_i^{\frac{\lambda\theta(\theta+1)}{1-\lambda\theta}} P_i^{-\theta-\frac{\lambda\theta^2}{1-\lambda\theta}} =& \bar{L}^{\frac{-\lambda\theta}{1-\lambda\theta}} \bar{A}_i^{\frac{\lambda\theta^2}{1-\lambda\theta}+\theta} \bar{\Gamma}_i^{\frac{-\theta}{1-\lambda\theta}} e^{\frac{-\mu_i\theta}{1-\lambda\theta}\text{weather}_i} \bar{l}_i^{\frac{\lambda\theta^2}{1-\lambda\theta}+\theta} y_i^{-\theta+1} \\
&+ \bar{L}^{-\frac{\lambda\theta}{1-\lambda\theta}} \sum_{j=1}^{N} \bar{A}_i^{\frac{\lambda\theta^2}{1-\lambda\theta}} \bar{t}_{ij}^{-\theta} \bar{\Gamma}_i^{\frac{-\theta}{1-\lambda\theta}} e^{\frac{-\mu_i\theta}{1-\lambda\theta}\text{weather}_i} \bar{l}_i^{\frac{\lambda\theta^2}{1-\lambda\theta}} P_j^{-\theta}
\end{aligned} \tag{29}
$$

To quantify the impact of a weather shock affecting ports infrastructure, I rely on the standard exact hat algebra approach and write the model in terms for changes from the equilibrium – using the notations $\hat{x}_i \equiv \frac{x_i'}{x_i}$ and $\Delta x_i \equiv x_i' - x_i$.

Consider a change in weather $\{\Delta\text{weather}_i\}_{i\in\mathcal{N}}$ and a change in trade deficits $\{\widehat{(1+\kappa_i)}\}_{i\in\mathcal{N}}$[16]. Given observed link traffic flows $\{\Xi_{ij}\}$, economic activity $\{Y_i, E_i\}$, and model parameters $\{\theta, \lambda, \mu_i\}$, the equilibrium change in economic outcomes $\{\hat{y}_i, \hat{P}_i\}$ is the solution of the following system of equations:[17]

$$
\begin{aligned}
\hat{y}_i^{\frac{1+\theta}{1-\lambda\theta}} \hat{P}_i^{\frac{-\theta}{1-\lambda\theta}+\theta} =& \left(\frac{E_i}{E_i + \sum_j \Xi_{ij}}\right) e^{\frac{-\mu_i\theta}{1-\lambda\theta}\Delta\text{weather}_i} \widehat{(1+\kappa_i)} \hat{y}_i \hat{P}_i^{\theta} \\
&+ \sum_{j=1}^{N} \left(\frac{\Xi_{ij}}{E_i + \sum_j \Xi_{ij}}\right) e^{\frac{-\mu_i\theta}{1-\lambda\theta}\Delta\text{weather}_i} \hat{y}_j^{\theta+1}
\end{aligned} \tag{30}
$$

$$
\begin{aligned}
\hat{y}_i^{\frac{\theta+1}{1-\lambda\theta}-(\theta+1)} \hat{P}_i^{\frac{-\theta}{1-\lambda\theta}} =& \left(\frac{Y_i}{Y_i + \sum_j \Xi_{ji}}\right) e^{\frac{-\mu_i\theta}{1-\lambda\theta}\Delta\text{weather}_i} \hat{y}_i^{-\theta} \\
&+ \sum_{j=1}^{N} \left(\frac{\Xi_{ji}}{Y_i + \sum_j \Xi_{ji}}\right) e^{\frac{-\mu_i\theta}{1-\lambda\theta}\Delta\text{weather}_i} \hat{P}_j^{-\theta}
\end{aligned} \tag{31}
$$

5 Estimation: Congestion and Weather Elasticities

There are two key elasticities to estimate to take to model to the data: the congestion elasticity and the weather elasticity. I can derive an estimation equation for them from the model microfoundations and take it to the shipping and weather data described above. Combining equations 23 and 24 leads to

$$
\text{time}_i = \Xi_i^{\delta_1} e^{-\delta_1\gamma\ \text{weather}_i} \omega_i^{\delta_1} \delta_i \tag{32}
$$

Building on Fuchs & Wong (2024), I consider the following estimation equation:

$$
\ln(\text{time}_{sit}) = \delta_1 \ln(\Xi_{i,[t-X;\,t]}) - \delta_1\gamma\ \text{weather}_{it} + \delta_{si} + \delta_t + \delta_{iy} + \epsilon_{sit} \tag{33}
$$

where s denotes a ship, i a port, t a day and y a year. time_{sit} is the dwell time experienced

[16] With a slight abuse of notation: $\widehat{(1+\kappa_i)} = \frac{1+\kappa_i'}{1+\kappa_i}$

[17] See Appendix A.6 for detailed derivation of the exact hat algebra equilibrium equations.

by ship s in port i on day t. $\Xi_{i,[t-X;\,t]}$ is a moving average of traffic at port i over the X days before t. I consider traffic over the past days to capture the potentially long-lasting effects of congestion – since it is increasing the dwell time, it might propagate to the next days. Similarly, $\text{weather}_{i,[t-X;\,t]}$ is a moving average of weather at port i over the X days before t. I also consider weather over the past days for several reasons: 1/ reduced-form evidence have shown that weather shocks can have effects lasting after the actual event (Figure C.3); 2/ since weather also affects dwell time indirectly through traffic (that is endogenous and depends on port costs, hence on local weather) and that I consider traffic over the past days, I also need to control for weather over this period. I add ship-port, port-year and day fixed-effects. The standard errors are two-way clustered at the ship and port levels. I set X = 14 days, but I find similar results using a longer time period for the moving averages (especially setting X = 28 as Fuchs & Wong 2024 do).

Following insights from reduced-form exercises, I measure weather with either wave height or water level. The weather measures considered will be used to compute counterfactuals under a climate change scenario: the objective is hence to have variables capturing the key changes in sea weather that will occur with climate change. To measure wave height, I use the share of days of the period where the port experiences extreme wave height (above 2m). This variable allows to account for the importance of extreme wave events, that will be increasing with climate change (Pörtner et al., 2019). The measure of water level considered is the mean total water level over the period, since total water level will be increasing in average with sea level rise (rather than a change in variability).

$$\text{weather}_{i,[t-X;\,t]} = \{\text{share days} > 2.0\text{m}\}_{i,[t-X;\,t]} \quad \text{or} \quad \text{weather}_{i,[t-X;\,t]} = \overline{\text{water level}}_{i,[t-X;\,t]}$$

I can also account for the possibility of adaptation to the change in weather. I rely on Carleton et al. (2022) and add an additional regressor by interacty short the run weather variable defined above with a long-run climate variable, the sample-period average of the weather variable:

$$\{\text{share days} > 2.0\text{m}\}_{i,[t-X;\,t]} \times \{\text{avg share days} > 2.0\text{m}\}_i \quad \text{or} \quad \overline{\text{water level}}_{i,[t-X;\,t]} \times \{\text{avg } \overline{\text{water level}}\}_i$$

I expect the coefficient of the weather variable to be positive, as bad weather increases port dwell time, but the coefficient of the weather $\times$ climate variable to be negative is there is adaptation to bad weather.

The measure of port traffic Ξ_{it} is defined as the number of ships present at the port i during day t, weighted by the share of the day the ships spend at the port[18] and by the ships capacity (vessel dead-weight tonnage).

[18] e.g. if a ship arrives very late in the day, it will not contribute as much to traffic this as a ship arrived very early in the day

There is an endogeneity issue with port traffic $\Xi_{i,[t-X;\,t]}$. The main threat to identification comes from potential reverse causality if the traffic is influenced by the time spent in port – for instance, when the dwell time begins to increase, ships might start to avoid the port, reducing traffic. Additionally, the unobserved shocks in the error term might affect both traffic and dwell time (productivity shocks for instance). To instrument for port traffic, I suggest use lagged port traffic: I consider port traffic at the exact same date, but one year before.

$$\mathbf{Z}_{i,[t-X;\,t]} = \ln(\Xi_{i,[t-X-1y;\,t-1y]}) \tag{34}$$

To be valid, this instrument needs to be relevant and exogenous. Relevance (i.e. $\mathbf{Z}$ correlated with Ξ) comes from seasonality in port traffic, see Figure **??**or the correlation between traffic on one day and traffic on the same day the year before at the port level. Exogeneity requires that $\mathbf{Z}$ is correlated with the dwell time solely through its correlation with congestion Ξ. There seems to be no channel through which previous year traffic could directly influence this year dwell time.

Results (without climate adaptation) are reported in Tables 5 and 6. For each weather variable (wave height and water level), I consider three specifications: including only weather among the regressors (column 1), including also traffic but not instrumenting for it (column 2), finally implementing the IV strategy (column 3). As expected, bad weather is associated with an increase in port dwell time. The OLS estimator of traffic elasticity is rather close to the one of Fuchs & Wong (2024) (I find 0.14 while there OLS estimate is 0.10), although I also include weather, consider a shorter moving average window and a more exhaustive set of ports. The instrument used in the IV specification seems sufficiently strong, as indicated by the high heteroskedasticity-robust Kleibergen-Paap rk Wald F statistic (KP-F). The IV value of traffic elasticity is exactly equal to the one found by Fuchs & Wong (2024) using a different instrument.

Results with climate adaptation are reported in Tables 7 and 8. The coefficients of weather elasticity get the expected signs: bad weather increases the port dwell time, but this effect is mitigated when the long term climate is worse. Both coefficients are significant for wave height and water level when not controlling for traffic (column 1); however, when adding traffic, the adaptation coefficient remains significative only for wave height. There seems to be heterogeneity consistent with adaptation for wave height, but not so much for total water level.

In appendix D, I show results when regressing on both wave height and water level (with or without adaptation). I find that when adding both regressors, water level effect is not significant anymore. The objective of these weather elasticities is to provide basis to compute climate change counterfactuals. According to climate predictions Pörtner et al. (2019), the change in water level will have a much higher magnitude than the change in wave height, due to sea level rise. This

Table 5: Effect of moving-average traffic and extreme wave height (2m) on port dwell time

	(1)	(2) OLS	(3) IV
share days wave height > 2m (MA)	0.08553***	0.07861***	0.07310***
	(0.01050)	(0.00916)	(0.00872)
log traffic (MA)		0.13742***	0.24665***
		(0.00635)	(0.03499)
date FE	✓	✓	✓
ship-port FE	✓	✓	✓
port-year FE	✓	✓	✓
# observations	6,114,910	6,114,910	6,114,910
# ships	11,311	11,311	11,311
# ports	1,620	1,620	1,620
First Stage KP-F			152.3

Standard errors in parentheses

* $p < 0.10$, ** $p < 0.05$, *** $p < 0.01$

Table 6: Effect of moving average traffic and water level on port dwell time

	(1)	(2) OLS	(3) IV
total water level (MA)	0.03165***	0.02185***	0.01407**
	(0.00676)	(0.00634)	(0.00675)
log traffic (MA)		0.13751***	0.24658***
		(0.00637)	(0.03507)
date FE	✓	✓	✓
ship-port FE	✓	✓	✓
port-year FE	✓	✓	✓
# observations	6,123,769	6,123,769	6,123,769
# ships	11,311	11,311	11,311
# ports	1,620	1,620	1,620
First Stage KP-F			156.7

Standard errors in parentheses

* $p < 0.10$, ** $p < 0.05$, *** $p < 0.01$

Table 7: Effect of moving average traffic and extreme wave height (2m) with adaptation on port dwell time

	(1)	(2) OLS	(3) IV
share days wave height >2m (MA)	0.12886***	0.11885***	0.11092***
	(0.01419)	(0.01239)	(0.01254)
share days wave height >2m (MA) × period-avg	-0.25700***	-0.23869***	-0.22419***
	(0.06433)	(0.05967)	(0.05964)
log traffic (MA)		0.13737***	0.24621***
		(0.00636)	(0.03506)
date FE	✓	✓	✓
ship-port FE	✓	✓	✓
port-year FE	✓	✓	✓
# observations	6,114,910	6,114,910	6,114,910
# ships	11,311	11,311	11,311
# ports	1,620	1,620	1,620
First Stage KP-F			152.6

Standard errors in parentheses

* $p < 0.10$, ** $p < 0.05$, *** $p < 0.01$

Table 8: Effect of moving average traffic and water level with adaptation on port dwell time

	(1)	(2) OLS	(3) IV
total water level (MA)	0.04178***	0.02849***	0.01796*
	(0.01035)	(0.00984)	(0.00975)
total water level (MA) × period-avg	-0.00622*	-0.00408	-0.00238
	(0.00372)	(0.00336)	(0.00331)
log traffic (MA)		0.13750***	0.24643***
		(0.00637)	(0.03507)
date FE	✓	✓	✓
ship-port FE	✓	✓	✓
port-year FE	✓	✓	✓
# observations	6,123,769	6,123,769	6,123,769
# ships	11,311	11,311	11,311
# ports	1,620	1,620	1,620
First Stage KP-F			156.3

Standard errors in parentheses

* $p < 0.10$, ** $p < 0.05$, *** $p < 0.01$

suggests that water level be first order compared to wave height. The preferred specification will hence be the one with water level (Table 6).

6 Sea Level Rise Counterfactuals

I now turn to counterfactuals. I first explain how I take the model to the data, then present the counterfactual exercises and their result.

6.1 Taking the model to the data

Structural parameters The estimation presented below allows to recover values of δ_1 and γ, related respectively to the congestion and weather elasticities. I turn to the literature to get values of other structural parameters. I rely on Allen & Arkolakis (2022) for the value of θ: I take $\theta = 8$ from Donaldson & Hornbeck (2016). I follow the same approach as Fuchs & Wong (2024) to set a value for δ_0, relying on Hummels & Schaur (2013): from their level-log elasticity of trade costs to transportation time, I derive a log-log elasticity of 0.4. Table 9 summarizes the parameters values used to compute the counterfactuals.

Table 9: Structural parameters values used in the counterfactuals computation

parameter	value	source
θ	8	Donaldson & Hornbeck (2016)
δ_0	0.4	Fuchs & Wong (2024); Hummels & Schaur (2013)
δ_1	0.25	estimation
λ	0.1	$\delta_0\delta_1$
γ	-0.02	estimation
μ	0.005	$-\gamma\delta_0\delta_1$

Port catchment areas I consider the top 400 container ports[19] and define their respective catchment areas. To do so, I start with a $0.25° \times 0.25°$ grid (representing cells of up to 30 km $\times$ 30 km at the Equator) covering all countries, weighted by population (CIESIN, 2018). Each grid cell is then assigned to the most relevant port based on the following rules:

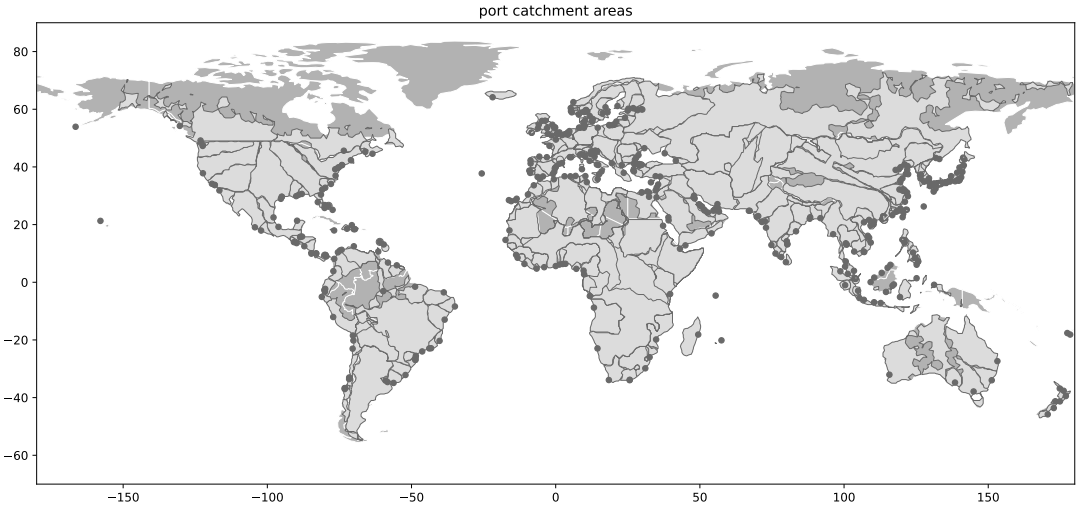
1. if the country has ports, the cell is allocated to the closest domestic port;
2. if the country is landlocked, the cell is allocated to the closest land-accessible foreign port.

These rules reflect a preference for domestic ports, even when a foreign port may be geographically closer. Distances are computed using the Open Route Service API (OpenRouteService,

[19]The raw AIS data contain many ports that are not adapted for containerships, or that are in fact technical stops for ships (for fuel, maintenance...) but not ports, etc. I use a cleaned version of the dataset to only look at point identified as container ports.

2025), which accounts for actual road networks rather than straight-line ("as-the-crow-flies") distances. This adjustment is crucial, especially in developing countries where sparse or indirect road networks can significantly increase travel distances. Additionally, I incorporate port importance into the catchment area calculation. Larger and better-equipped ports may attract more exports and imports, even when farther away. To account for this, I use total entering port calls over the 2015–2023 period as a proxy for port importance and adjust distances accordingly. Specifically, I scale the road distance to each port by $1/\sqrt{\text{port importance}}$. This formulation implies that if two ports are at the same location but one is twice as large as the other, its catchment area will be twice as extensive.[20] With this procedure, I compute port catchment areas, i.e. shares of land related to each port, plotted in Figure 6. A port catchment area can cover only a part of a country (e.g. French ports cover each one a share of French territory), a whole country or even several countries (e.g. the port of Calcutta catchment area covers part of India but also Nepal and Bhutan).

Figure 6: Port catchment areas worldwide



Note: Ports are plotted as dark dots, and port catchment areas are plotted as gray areas delimited by dark lines. The catchment area of a given port is the area in which this port is located. Parts of the world belong to no port catchment area because they have no road network to connect them to ports (e.g. the Amazon rainforest).

Outcome, expenditure, and traffic From the port catchment areas, I can compute the population-weighted shares of each country c related to each port i, $\omega_{c,i}$. I then rely on Penn World Tables to get country-level outcome Y_c and expenditure E_c for the year 2019. From these, I build port-level outcome $Y_i = \sum_c \omega_{c,i} Y_c$, representing the amount of goods produced by firms that export through port i (that can come from different countries); and port-level expenditure

[20] For example, without adjusting for port importance, I find that only 1% of Chinese exports would go through Shanghai, despite it being the world's largest port, because it is located in a region with many other ports. Incorporating port importance corrects for this distortion.

$E_i = \sum_c \omega_{c,i} E_c$, representing the amount of goods consumed by agents that import through port i (coming from potentially different countries as well).

To solve the exact hat algebra system of equations 30 and 30, I additionally require to observe traffic flows Ξ_{ij}. I take them from AIS shipping data, considering the shipping links that have more than 50 calls over the year 2019, between the 400 ports I take into account. For these links, I measure traffic Ξ_{ij} as the number of ships (weighted by their capacity) traveling on the link during the year 2019.

Outcome effects With these data and structural parameters values, I can compute the effects on endogenous variables of a given weather shock $\{\Delta\text{weather}_i\}_{i\in\mathcal{N}}$ following the exact hat algebra system of equations 30 and 31. I take trade deficits into account using a two-step procedure (Ossa, 2016). I first compute counterfactual outcomes assuming no weather shock but taking the trade deficits to zero; then I compute counterfactuals with a weather change assuming the trade deficits stay to zero. The effect of the change in weather is computed as the difference between equilibrium levels in the two counterfactuals. This procedure is detailed in Appendix E. To solve the system of equations, I use a fixed point algorithm (adapted from the one of Allen & Arkolakis 2022, see Appendix F).

I retrieve the equilibrium changes in nominal economic outcome $\{\hat{y}_i\}_{i\in\mathcal{N}}$ and price index $\{\hat{P}_i\}_{i\in\mathcal{N}}$ at the port catchment area level, from which I can derive changes in real outcome $\{\hat{y}_i/\hat{P}_i\}_{i\in\mathcal{N}}$ – the reference welfare metric used by Arkolakis et al. (2012). To better understand the mechanisms leading to these welfare effects, I also look at the changes in port traffic $\{\hat{\Xi}_i\}_{i\in\mathcal{N}}$ and route traffic $\{\hat{\Xi}_{ij}\}_{i,j\in\mathcal{N}}$.

6.2 Predicted vs observed trade flows

As in Allen & Arkolakis (2022), there is a close link in the model between the gravity equation for trade flows (equation 9) and the gravity equation of traffic on links (equation 20). Combining these equations allows to write an expression of equilibrium trade flows as:[21]

$$X_{ij} = Y_i \times c_{ij}^X \times E_j \tag{35}$$

where c_{ij}^X is the (i,j)-th element of the matrix $\mathbf{C}^{\mathbf{X}} \equiv \left(\mathbf{D}^{\mathbf{X}} - [\Xi_{ij}]\right)^{-1}$, where $\mathbf{D}^{\mathbf{X}}$ is a diagonal matrix with i-th element equal to $d_i^X \equiv \frac{1}{2}\left(Y_i + E_i\right) + \frac{1}{2}\left(\sum_j \Xi_{ij} + \Xi_{ji}\right)$.

[21] See Appendix A.4 for detailed derivation of the relationship between trade flows and traffic flows.

Following Allen & Arkolakis (2022), this expression for traffic flows between locations i and j depends only on available data. It allows to build a *prediction* of trade flows based on the model, that we can then compare with *observed* trade flows from data, to check the validity of the model.

I rely on traffic flows between ports which catchment area does not cover several countries. From the traffic flows Ξ_{ij}, the outcome Y_i and expenditure E_i of those ports, I can predict trade flows at the *port level* X_{ij} using equation 35. I then aggregate ports to the country they belong to, to get predicted trade flows of the *country level* $X_{c,c'}$. I compare these model-precicted trade flows with bilateral trade flows data at the country level from Mayer et al. (2023) and Fontagné et al. (2023) in 2019 (aggregating all manufacturing and agriculture sectors together).[22]

Figure 7: Predicted trade flows using traffic compared to observed trade flows

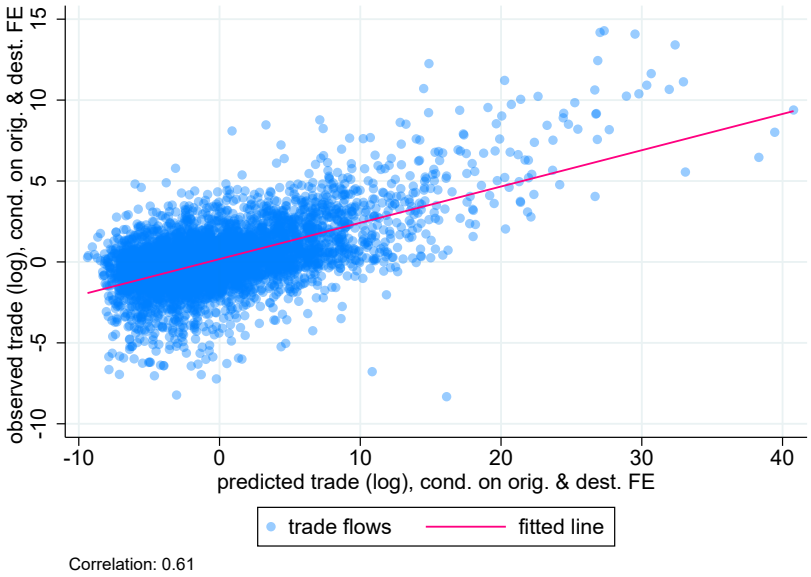


Figure 7 shows the scatter plot between observed and predicted log trade flows, conditional on origin and destination fixed effects.[23] The strong positive correlation (0.61) indicates that the traffic matrix is efficient in predicting the trade flows. This suggests the model is performing well to describe international trade flows with a shipping network, extending the result of Allen & Arkolakis (2022) showing that their original model performs well to describe trade between

[22] Mayer et al. (2023) and Fontagné et al. (2023) combine data on annual cross-border international bilateral flows (UN Commodity Trade Statistics Database (COMTRADE) for manufacturing and Food and Agriculture Organization of the United Nations Statistics Division (FAOSTAT) for agriculture) with production data (the UNIDO Industrial Statistics database (INDSTAT) for manufacturing and again FAOSTAT for agriculture) to compile a square matrix of bilateral trade flows for each sector, including self-trade.

[23] As Allen & Arkolakis (2022) notice, controlling for origin country and destination fixed effects allows that the variation arises only from the bilateral flows and not from characteristics of origin or destination countries such as income.

cities in US with a road network.

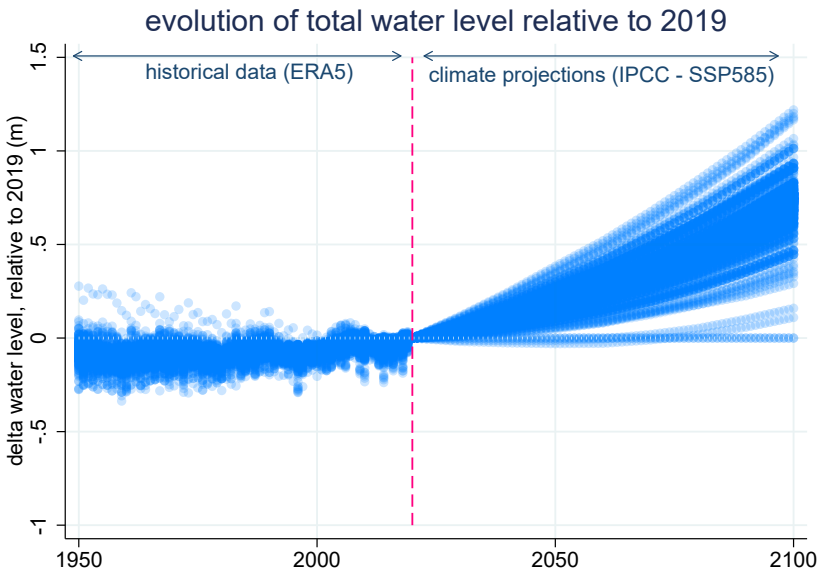
6.3 Counterfactuals: Sea Level Rise

I look at the effect of a global climate shock: sea level rise. In the coming years, all ports will experience a change in their water level; however, these changes will be heterogeneous, some ports will experience a much more important rise in water level than others (Pörtner et al., 2019). I compute the future water level at each port location using IPCC sea level projections (Garner et al., 2022) under the SSP5-8.5 scenario (very high GHG emissions). The counterfactual exercise computes the effects of the change in water level between 2019 and 2100 under this scenario.

$$\Delta\text{weather}_i = \text{water level}_{i,2019} - \text{water level}_{i,2100} \tag{36}$$

Figure 8 illustrates the changes in water level compared to 2019 at the different port locations. There is significant heterogeneity across ports: while some ports are expected to experience virtually no change in water level, most of the ports will experience sea level rise, up to +1.3m in 2100. Comparing these projections of future sea level rise after 2019 to realized sea level rise before 2019 from historical data, one can notice the acceleration in rising water level.

Figure 8: Evolution of water level in ports compared, using historical and projection data

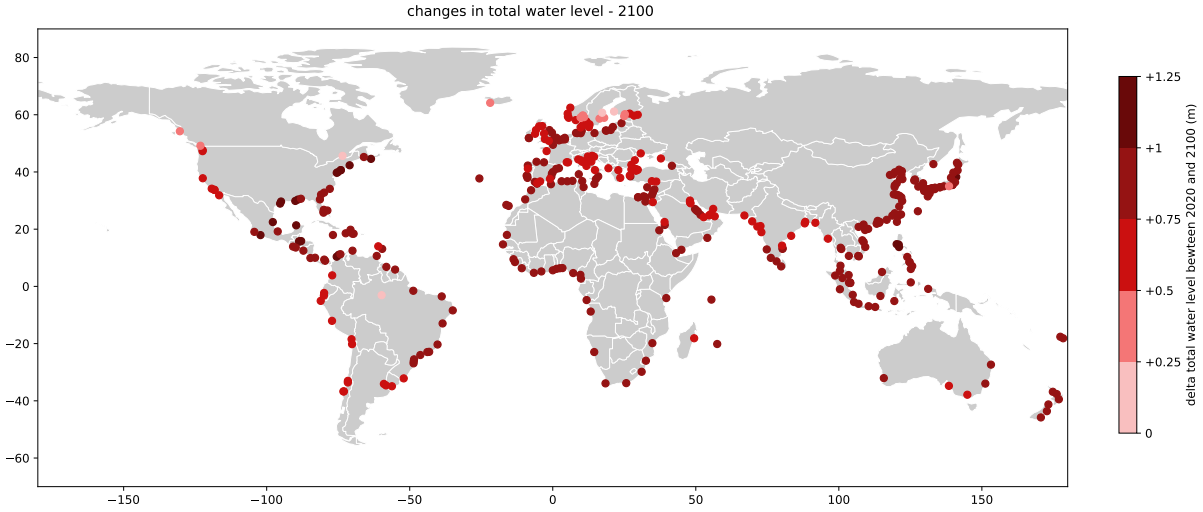


Note: each dot represents the change in total water level in one port, compared to 2019. Before 2019, the values are observed in ERA5 data. After 2019, the values are predicted by IPCC following the SSP5-8.5 scenario.

Figure 9 shows the spatial distribution of the changes in water level between 2019 and 2100. Some of the less affected ports locate in Northern Europe (Sweden, Norway, Finland) while the

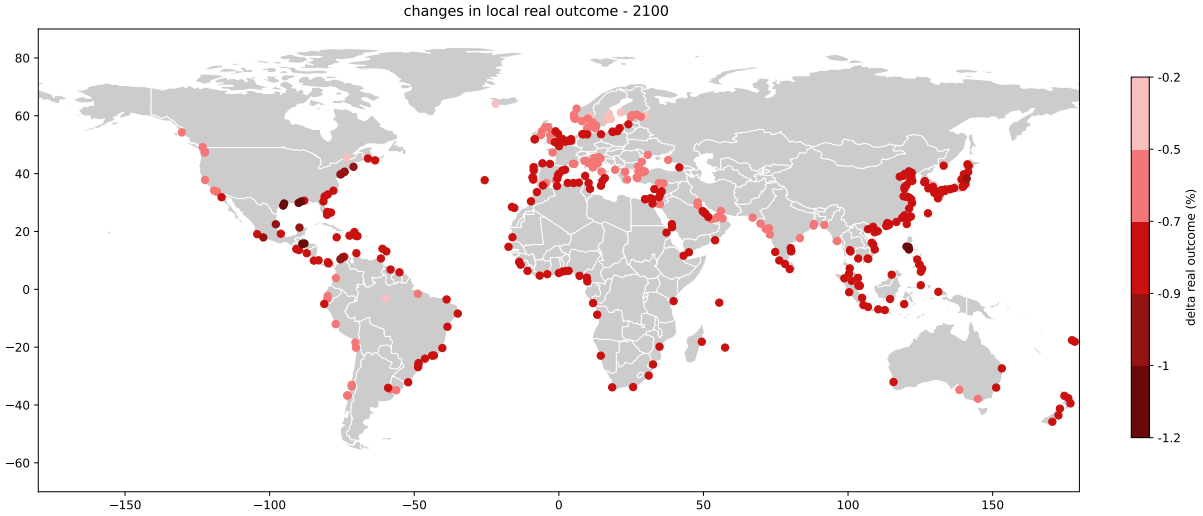
most affected ports are in the the Philippines and East Coast of the USA. The map also shows the significant spatial correlation of the sea level rise: ports in the same area are facing similar levels of water level increase.

Figure 9: Changes in port water level between 2019 and 2100 under scenario SSP5-8.5



The changes in local real outcome $\hat{y}_i/\hat{P}_i$ (i.e. welfare changes, Arkolakis et al. 2012) predicted by the model are presented in Figure 10. Ports loose up to 1.1% of real outcome, in Freeport (USA), New Orleans (USA), Subic Bay (Philippines), Manila (Philippines). The lowest impact is at -0.2% real outcome (Gavle, Sweden; Rauma, Finland).

Figure 10: Changes in port real outcome between 2019 and 2100 under scenario SSP5-8.5



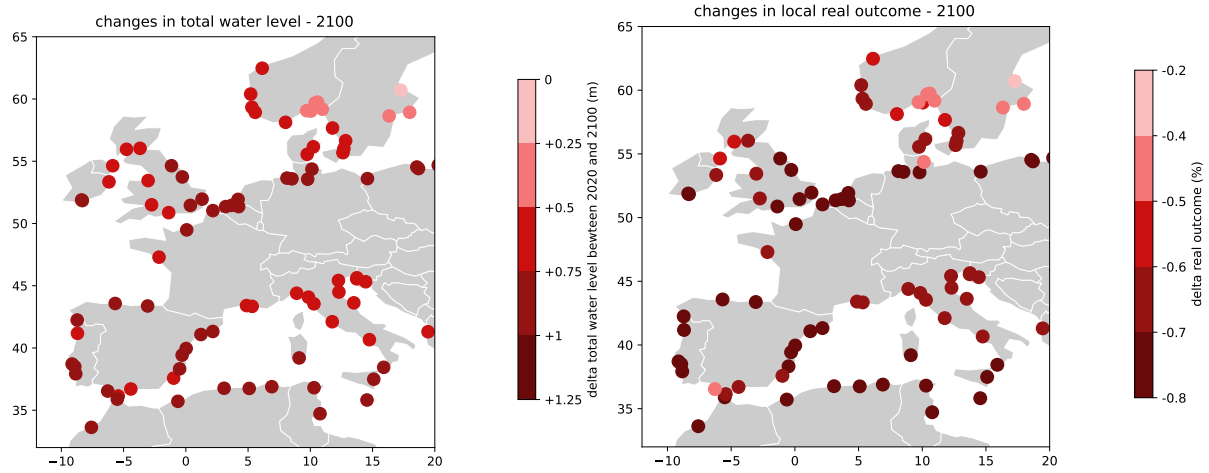
The distribution of local water level and real outcome changes for different years can be found

in appendix G. The distribution of welfare loss widens with time.

Comparing maps 9 and 10, we see a correlation between the levels of water level increase and real outcome decrease: for instance, Northern Europe ports are among the less subject to sea level rise, and also suffer less welfare loss; quite the opposite, the Gulf of Mexico will experience both heavy sea level rise and welfare loss.

However, the mapping between local weather change and local welfare loss is not perfect. Looking closer at Europe (Figure 11), one can see ports with similar changes in water level (left panel) experiencing different changes in real outcome (right panel). For instance in Spain, the ports of Cadix and Barcelona experience very similar change in water level (resp. +0.80m and +0.81m) but quite different changes in real outcome (resp. -0.44% and -0.74%). This suggests that the impact of climate change on a given port cannot be determined by its own water level rise only (*direct* effect), spillovers from other ports (*indirect* effect) play a significant role.

Figure 11: Changes in water level and real outcome in 2100 – zoom on Europe

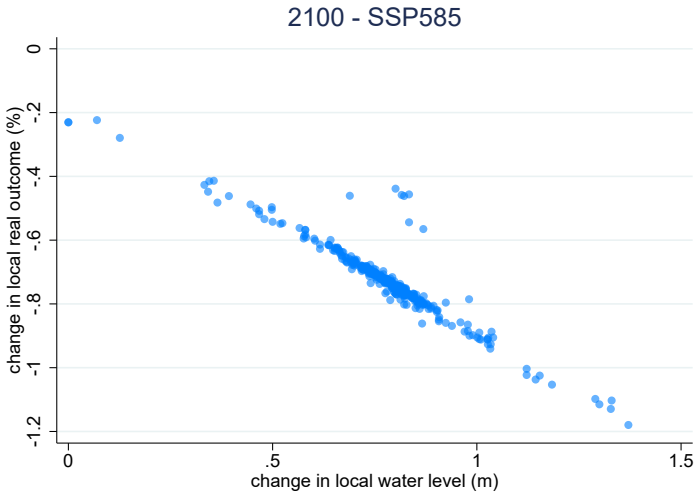


(a) change in water level

(b) change in real outcome

Figure 12 highlights these spillover effects coming from other ports. There is a indeed a very strong correlation between a port's own change in local water and change in real outcome. However, it is worth noticing that the intercept of this damage function is not null: ports facing no change in water level still get a loss of real outcome of about 0.2%. This means that they have no *direct* effect from sea level rise (since no change in water level), but only *indirect* effects.

Figure 12: Scatter plot: changes in water level and real outcome in 2100



7 Towards a flexible network

The container-shipping network is sparse – meaning that not all pairs of ports are connected by a direct shipping link. Over the main 400 ports, I observe in the shipping data only 3,755 active links. In other words, the adjacency matrix, describing the direct connections between ports, has many zeros.[24] This feature is common to other transportation networks, like railroads or highways. The key difference of the shipping network with terrestrial transportation networks studied in the literature, is that this adjacency matrix is way more flexible. Indeed, it is much easier to create a new link or to delete an existing one in a shipping network, since its requires no infrastructure investment: there is no road to build, this is open sea. The fixed cost for shipping links is much less important than for terrestrial transportation networks. The adjacency matrix is hence much more likely to evolve over time. In the shipping data, it appears that only 40% of the links observed in the network are active over the whole period (see Figure H.8): we often see links opening and closing.

So far, I have considered the shipping network structure as fixed: the set of existing links remains unchanged, there is only reallocation of traffic within these existing links. However, it seems reasonable to think that with sea level rise and the major disruptions induced in ports, the shipping network structure will evolve: shipping companies might not continue to serve ports that are under water.

Over the data period (2015-2023), I observe limited empirical evidence that the network structure as already reacted to the weather conditions of ports: I find that weather shocks in a

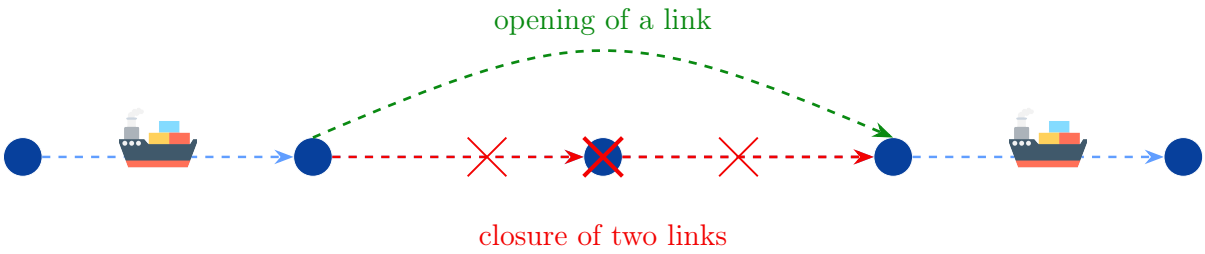
[24] Precisely, 98% of its coefficients are zero: the container-shipping network is *very* sparse.

port lead to a marginal (yet significant) reduction of its number of active links (see Appendix H). Yet, this mechanism might still be important to take into account over the long run. First, because the support of weather shocks is expected to change in the coming years (Pörtner et al., 2019): ports have not experienced dramatic changes in their weather conditions over the 10 years of data, but they will likely do so in the future with sea level rise (see Figure 8). Second, from a normative point of view, the evolution of the shipping network structure can be an adaptation mechanism helping to mitigate the impact of climate change. Under this perspective, network adaptation *should* be happening, even though we might not yet see it implemented.

To show the potential mitigation through network adaptation, I conduct a proof of concept exercise. In a thought experiment scenario, I consider a shock affecting only one port, and look at the welfare effects with and without network flexibility. In the first case, without network adaptation, I consider a weather shift in the port of Jakarta only, and compute counterfactuals using the mode presented above – so only allowing for traffic reallocation within the network. In the second case, I further allow links to open and to close after Jakarta's port shock, and then compute counterfactuals using the model after this network adaptation. This exercise gives two general equilibrium effects, with and without link adaptation. Comparing them will inform on the ability of network flexibility to act as a mitigation mechanism.

To determine which links are the most likely to open or close when the port of Jakarta is down, I rely on the literature analyzing shipping network response to Covid shock in ports. Dirzka & Acciaro (2022) explain than when a port was not operational because of lockdown during the Covid period, ship operators could cancel a service commitment by omitting a port call. By doing so, they would delete two links and open a new one, as explained in Figure 13.

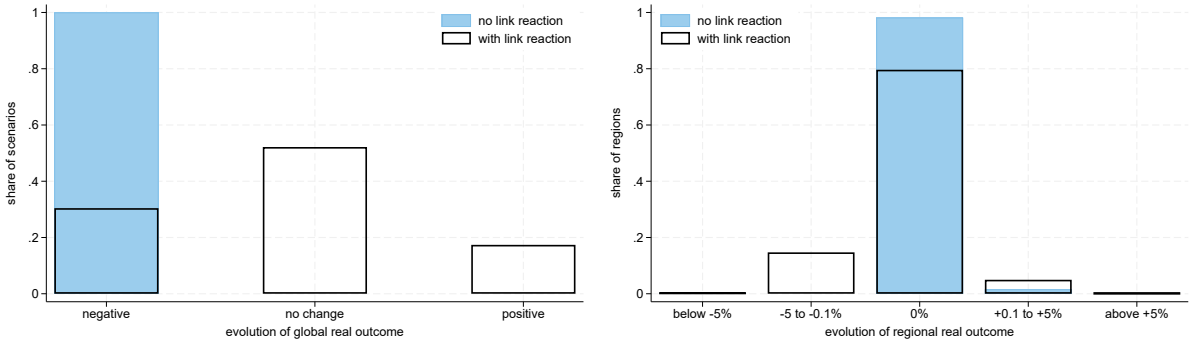
Figure 13: Port call omission mechanism and resulting links closure and opening



I apply this mechanism to the port of Jakarta by identifying 23 services with low traffic (below median)[25] and by omitting the port of Jakarta for each of these services successively. I then get 23 replications of the exercise, each time with a different network adaptation. The results of this exercise are presented in Figure 14. The left panel depicts the effects on global welfare (real outcome). The blue bar represents the effect of the shock on global welfare without

[25]Services with high traffic are less likely to be changed.

Figure 14: Effect of Jakarta port shock on real outcome, with and without network adaptation



(a) effect on global real outcome

(b) effect on port real outcome

network adaptation: as expected, the effect is negative. The black bars represent the effects with different version of network adaptation. Some alternative networks still lead to a negative global welfare effect; but some lead to a complete alleviation of the shock, while others even improve global welfare.

These results were obtained for had hoc adaptations of the shipping network: they shows that network adaptation *can* alleviate the negative effect of a port shock on global real outcome, hence acting as a mitigation tool. Work in progress is to determine how the shipping network might actually evolve, as the result of a decision from a shipping sector.

8 Conclusion

I examine the economic impact of weather shocks affecting port infrastructures in the shipping network. I focus on the port congestion created by adverse weather conditions, that increases the cost of port services for ships. The framework provided allows to understand the spillovers mechanisms created by the network structure of shipping: the port inter-linkages spread the effect of local weather shocks, generating potential ripple effects – but also substitution mechanisms. A policy implication of this work is about infrastructures decisions to protect ports against sea level rise (Christodoulou et al., 2019): some ports are particularly critical for global welfare, and several countries would benefit from their protection.

References

Allen, T. & Arkolakis, C. (2014). Trade and the topography of the spatial economy. *The Quarterly Journal of Economics*, 129(3), 1085–1140.

Allen, T. & Arkolakis, C. (2022). The welfare effects of transportation infrastructure improvements. *The Review of Economic Studies*, 89(6), 2911–2957.

Anderson, J. E. & Van Wincoop, E. (2003). Gravity with gravitas: A solution to the border puzzle. *American economic review*, 93(1), 170–192.

Arkolakis, C., Costinot, A., & Rodríguez-Clare, A. (2012). New trade models, same old gains? *American Economic Review*, 102(1), 94–130.

Balboni, C., Boehm, J., & Waseem, M. (2023). Firm adaptation and production networks: Structural evidence from extreme weather events in pakistan.

Becker, A., Ng, A. K., McEvoy, D., & Mullett, J. (2018). Implications of climate change for shipping: Ports and supply chains. *Wiley Interdisciplinary Reviews: Climate Change*, 9(2), e508.

Brancaccio, G., Kalouptsidi, M., & Papageorgiou, T. (2020). Geography, transportation, and endogenous trade costs. *Econometrica*, 88(2), 657–691.

Brancaccio, G., Kalouptsidi, M., & Papageorgiou, T. (2024). Investment in infrastructure and trade: The case of ports. *National Bureau of Economic Research Working Paper*.

Carleton, T., Crews, L., & Nath, I. (2023). *Agriculture, trade, and the spatial efficiency of global water use*. Technical report, Working paper.

Carleton, T., Jina, A., Delgado, M., Greenstone, M., Houser, T., Hsiang, S., Hultgren, A., Kopp, R. E., McCusker, K. E., Nath, I., et al. (2022). Valuing the global mortality consequences of climate change accounting for adaptation costs and benefits. *The Quarterly Journal of Economics*, 137(4), 2037–2105.

Christodoulou, A., Christidis, P., & Demirel, H. (2019). Sea-level rise in ports: a wider focus on impacts. *Maritime Economics & Logistics*, 21, 482–496.

CIESIN (2018). Gridded population of the world, version 4.11 (gpwv4): Population count. Revision 11. Palisades, NY: NASA Socioeconomic Data and Applications Center (SEDAC).

Costinot, A., Donaldson, D., & Smith, C. (2016). Evolving comparative advantage and the impact of climate change in agricultural markets: Evidence from 1.7 million fields around the world. *Journal of Political Economy*, 124(1), 205–248.

Costinot, A. & Rodríguez-Clare, A. (2014). Trade theory with numbers: Quantifying the consequences of globalization. In *Handbook of international economics*, volume 4 (pp. 197–261). Elsevier.

Dell, M., Jones, B. F., & Olken, B. A. (2012). Temperature shocks and economic growth: Evidence from the last half century. *American Economic Journal: Macroeconomics*, 4(3), 66–95.

Deryugina, T., Kawano, L., & Levitt, S. (2018). The economic impact of hurricane katrina on its victims: Evidence from individual tax returns. *American Economic Journal: Applied Economics*, 10(2), 202–233.

Dirzka, C. & Acciaro, M. (2022). Global shipping network dynamics during the covid-19 pandemic's initial phases. *Journal of transport geography*, 99, 103265.

Donaldson, D. & Hornbeck, R. (2016). Railroads and american economic growth: A "market access" approach. *The Quarterly Journal of Economics*, 131(2), 799–858.

Dube, A., Girardi, D., Jorda, O., & Taylor, A. M. (2023). *A local projections approach to difference-in-differences event studies*. Technical report, National Bureau of Economic Research.

Eaton, J. & Kortum, S. (2002). Technology, geography, and trade. *Econometrica*, 70(5), 1741–1779.

Fajgelbaum, P. D. & Schaal, E. (2020). Optimal transport networks in spatial equilibrium. *Econometrica*, 88(4), 1411–1452.

Fontagné, L., Lebrand, M. S. M., Murray, S., Santoni, G., & Ruta, M. (2023). Trade and infrastructure integration in africa. *Available at SSRN 4672520*.

Fuchs, S. & Wong, W. F. (2024). Multimodal transport networks. *Mimeo*.

Ganapati, S., Wong, W. F., & Ziv, O. (2021). Entrepot: Hubs, scale, and trade costs. *National Bureau of Economic Research Working Paper*.

Garner, G., Hermans, T. H., Kopp, R., Slangen, A., Edwards, T., Levermann, A., Nowicki, S., Palmer, M. D., Smith, C., Fox-Kemper, B., et al. (2022). Ipcc ar6 wgi sea level projections.

Gouel, C. & Laborde, D. (2021). The crucial role of domestic and international market-mediated adaptation to climate change. *Journal of Environmental Economics and Management*, 106, 102408.

Heiland, I., Moxnes, A., Ulltveit-Moe, K. H., & Zi, Y. (2019). Trade from space: Shipping networks and the global implications of local shocks. *CEPR Discussion Paper No. DP14193*.

Hersbach, H., Bell, B., Berrisford, P., Biavati, G., Horányi, A., Sabater, J. M., Nicolas, J., Peubey, C., Radu, R., Rozum, I., et al. (2023). Era5 hourly data on pressure levels from 1940 to present: Tech. rep.

Hummels, D. L. & Schaur, G. (2013). Time as a trade barrier. *American Economic Review*, 103(7), 2935–2959.

Izaguirre, C., Losada, I. J., Camus, P., Vigh, J. L., & Stenek, V. (2021). Climate change risk to global port operations. *Nature Climate Change*, 11(1), 14–20.

Ludwig, P. (2024). Can unilateral policy decarbonize maritime trade?

Mayer, T., Santoni, G., & Vicard, V. (2023). *The CEPII trade and production database*. CEPII.

OpenRouteService (2025). Openrouteservice api documentation. https://openrouteservice.org. Heidelberg Institute for Geoinformation Technology. Accessed: 2025-02-26.

Ossa, R. (2016). Quantitative models of commercial policy. In *Handbook of commercial policy*, volume 1 (pp. 207–259). Elsevier.

Pörtner, H.-O., Roberts, D. C., Masson-Delmotte, V., Zhai, P., Tignor, M., Poloczanska, E., Weyer, N., et al. (2019). The ocean and cryosphere in a changing climate. *IPCC special report on the ocean and cryosphere in a changing climate*, 1155, 10–1017.

UNCTAD (2023). *Review of Maritime Transport*. Technical report.

Wang, D., Guan, D., Zhu, S., Kinnon, M. M., Geng, G., Zhang, Q., Zheng, H., Lei, T., Shao, S., Gong, P., et al. (2021). Economic footprint of california wildfires in 2018. *Nature Sustainability*, 4(3), 252–260.

Appendix

A Model derivations

A.1 Equilibrium equations

Combining equations 6 and 9 yields (using additionally that $Y_i = w_i L_i$):

$$\Pi_i = \bar{A}_i l_i y_i^{-\frac{\theta+1}{\theta}} \bar{L}^{1-\frac{\theta+1}{\theta}} \tag{A.1}$$

The market clearing condition $Y_i = \sum_j X_{ij}$ from 8 can be rewritten using 9 as

$$\Pi_i^{-\theta} = \sum_j \tau_{ij}^{-\theta} E_j P_j^{\theta} \tag{A.2}$$

With the unbalanced trade assumption 11, I can write the first equilibrium equation:

$$\bar{A}_i^{-\theta} \bar{l}_i^{-\theta} y_i^{1+\theta} = \sum_j \tau_{ij}^{-\theta} (1+\kappa_j) y_j P_j^{\theta} \tag{A.3}$$

Similarly, combining the market clearing condition $E_i = \sum_j X_{ji}$ from 8 with 9 yields

$$P_i^{-\theta} = \sum_j \tau_{ji}^{-\theta} Y_j \Pi_j^{\theta} \tag{A.4}$$

Here no need to account for deficit, it directly leads to the second equilibrium equation:

$$P_i^{-\theta} = \sum_j \tau_{ji}^{-\theta} \bar{A}_j^{\theta} \bar{l}_j^{\theta} y_j^{-(\theta+1)} \tag{A.5}$$

A.2 Transportation costs

Starting from $\tau_{ij}^{-\theta} = \sum_{r \in \mathcal{R}_{ij}} \left(\prod_{l=0}^{K} p_{r_l}^{-\theta} \right) \left(\prod_{l=1}^{K} t_{r_{l-1}, r_l}^{-\theta} \right)$ (coming from equation 7), I follow A&A into enumerating all the possible routes going from i to j of length K :

$$\tau_{ij}^{-\theta} = \sum_{K=0}^{+\infty} \left(\sum_{k_1=1}^{N} \sum_{k_2=1}^{N} \dots \sum_{k_{K-1}=1}^{N} p_i^{-\theta} t_{i,k_1}^{-\theta} p_{k_1}^{-\theta} t_{k_1,k_2}^{-\theta} \dots p_{k_{K-1}}^{-\theta} t_{k_{K-1},j}^{-\theta} p_j^{-\theta} \right) \tag{A.6}$$

I then adapt the matrix algebra of A&A to simplify this expression. In equation A.6, one can group an origin port with the link after, i.e. consider $g_{ij} \equiv p_i^{-\theta} t_{ij}^{-\theta}$. In which case,

$$\tau_{ij}^{-\theta} = \sum_{K=0}^{+\infty} (\mathbf{G}^K)_{ij} \, p_j^{-\theta} \quad \text{then} \quad \sum_{K=0}^{+\infty} \mathbf{G}^K = (\mathbf{I} - \mathbf{G})^{-1} \equiv \mathbf{C}^G \quad \Rightarrow \quad \tau_{ij}^{-\theta} = c_{ij}^G \, p_j^{-\theta} \tag{A.7}$$

Another alternative to simplify equation A.6 is to group an origin port with the link before, i.e. consider $d_{ij} \equiv t_{ij}^{-\theta} p_j^{-\theta}$. Then,

$$\tau_{ij}^{-\theta} = \sum_{K=0}^{+\infty} (\mathbf{D}^K)_{ij}\, p_i^{-\theta} \quad \text{then} \quad \sum_{K=0}^{+\infty} \mathbf{D}^K = (\mathbf{I} - \mathbf{D})^{-1} \equiv \mathbf{C}^D \quad \Rightarrow \quad \tau_{ij}^{-\theta} = c_{ij}^D\, p_i^{-\theta} \tag{A.8}$$

Equations A.7 and A.8 provide two alternative analytical relationships between transportation network and transportation costs.

A.3 Traffic Gravity equations

Let π_{ij}^k denote the expected number of times in which a node k is used in trade between i and j, π_{ij}^k:

$$\pi_{ij}^k = \sum_{r \in \mathcal{R}_{ij}} \left(\frac{\pi_{ij,r}}{\sum_{r' \in \mathcal{R}_{ij}} \pi_{ij,r'}} \right) n_r^k \tag{A.9}$$

where n_r^k is the number of times the route r passes through node k. Combining with equation 5 yields:

$$\pi_{ij}^k = \tau_{ij}^{\theta} \left(\sum_{r \in \mathcal{R}_{ij}} \left(\prod_{l=0}^{K} p_{r_l}^{-\theta} \right) \left(\prod_{l=1}^{K} t_{r_{l-1},r_l}^{-\theta} \right) \right) n_r^k$$

I then enumerating explicitly all possible routes going from i to j through k. Routes can have different lengths K (equal to the number of links, or the number of ports -1). A route of length K can go through node k at position $B \in \{0, 1, ..., K\}$. Isolating the cost on the left of k and the cost on the right of k leads to:

$$\pi_{ij}^k = \tau_{ij}^{\theta} \sum_{K=0}^{\infty} \sum_{B=0}^{K-1} \left(\sum_{r \in \mathcal{R}_{ik,B}} \prod_{n=1}^{B} g_{r_{n-1},r_n} \right) p_k^{-\theta} \left(\sum_{r \in \mathcal{R}_{kj,K-B}} \prod_{n=1}^{K-B} d_{r_{n-1},r_n} \right)$$

Using the same computation tricks as above:

$$\pi_{ij}^k = \tau_{ij}^{\theta} \sum_{K=0}^{\infty} \sum_{B=0}^{K-1} (\mathbf{G}^B)_{ij}\, p_k^{-\theta}\, (\mathbf{D}^{K-B})_{ij} \tag{A.10}$$

With some matrix algebra, one can show that

$$\sum_{K=0}^{+\infty} \sum_{B=0}^{K-1} \mathbf{G}^B\, \mathbf{P}\, \mathbf{D}^{K-B} = (\mathbf{I} - \mathbf{G})^{-1}\, \mathbf{P}\, (\mathbf{I} - \mathbf{D})^{-1}$$

Using the notations from the equations A.7 and A.8:

$$\pi_{ij}^{k} = \frac{c_{ik}^{G}\, p_{k}^{-\theta}\, c_{kj}^{D}}{\tau_{ij}^{\theta}} = \frac{\tau_{ik}^{-\theta}\, p_{k}^{\theta}\, \tau_{kj}^{-\theta}}{\tau_{ij}^{\theta}} \tag{A.11}$$

Let Ξ_k be the node traffic in location k, i.e. the value of all goods going through node k (either because they have k as an origin or destination, or just because they transit through k as an intermediate node along their route):

$$\Xi_k = \sum_{i \in \mathcal{N}} \sum_{j \in \mathcal{N}} \pi_{ij}^{k} X_{ij} \tag{A.12}$$

Substituting for X_{ij} with equation 9, I find that equation A.12 can be written as gravity equation for node traffic, with the same market access terms as a the gravity equation for trade flows 9:

$$\Xi_k = p_k^{\theta} \times P_k^{-\theta} \times \Pi_k^{-\theta} \tag{A.13}$$

A&A also show that similarly, link traffic Ξ_{kl} can be expressed with a gravity equation for link traffic:

$$\pi_{ij}^{kl} = \frac{\tau_{ik}^{-\theta}\, t_{kl}^{-\theta}\, \tau_{lj}^{-\theta}}{\tau_{ij}^{\theta}} \tag{A.14}$$

$$\Xi_{kl} = t_{lk}^{-\theta} \times P_k^{-\theta} \times \Pi_l^{-\theta} \tag{A.15}$$

A.4 Traffic and trade

Writing equation 9 in matrix notations – where $[x_{ij}]$ denotes a $N \times N$ matrix of general term x_{ij}, and $\text{diag}\,(x_i)$ a $N \times N$ diagonal matrix where the diagonal term of the i-th row is equal to x_i:

$$[X_{ij}] = \text{diag}\left(\frac{Y_i}{\Pi_i^{-\theta}}\right) \left[\tau_{ij}^{-\theta}\right] \text{diag}\left(\frac{E_i}{P_i^{-\theta}}\right) \tag{A.16}$$

Combining with equation A.8, it yields

$$[X_{ij}] = \text{diag}\left(\frac{Y_i}{\Pi_i^{-\theta}} p_i^{-\theta}\right) (\mathbf{I} - \mathbf{D})^{-1} \text{diag}\left(\frac{E_i}{P_i^{-\theta}}\right) \tag{A.17}$$

with

$$\mathbf{D} = [d_{ij}] = \left[\tau_{ij}^{-\theta}\right] \text{diag}\left(p_i^{-\theta}\right)$$

It comes

$$[X_{ij}] = \text{diag}\left(\frac{Y_i}{\Pi_i^{-\theta}} p_i^{-\theta}\right) \left(\mathbf{I} - \left[\tau_{ij}^{-\theta}\right] \text{diag}\left(p_i^{-\theta}\right)\right)^{-1} \text{diag}\left(\frac{E_i}{P_i^{-\theta}}\right) \tag{A.18}$$

Similarly, writing equation 20 in matrix notations:

$$[\Xi_{ij}] = \text{diag}\left(P_i^{-\theta}\right)\left[t_{ij}^{-\theta}\right]\text{diag}\left(\Pi_i^{-\theta}\right) \tag{A.19}$$

Inverting, it comes:

$$\left[t_{ij}^{-\theta}\right] = \text{diag}\left(P_i^{\theta}\right)[\Xi_{ij}]\,\text{diag}\left(\Pi_i^{\theta}\right) \tag{A.20}$$

Combining equations A.18 and A.20:

$$[X_{ij}] = \text{diag}\left(\frac{Y_i}{\Pi_i^{-\theta}}p_i^{-\theta}\right)\left(\mathbf{I} - \text{diag}\left(P_i^{\theta}\right)[\Xi_{ij}]\,\text{diag}\left(\Pi_i^{\theta}\right)\text{diag}\left(p_i^{-\theta}\right)\right)^{-1}\text{diag}\left(\frac{E_i}{P_i^{-\theta}}\right) \tag{A.21}$$

Inverting the matrices:

$$[X_{ij}]^{-1} = \text{diag}\left(E_i^{-1}\right)\left(\text{diag}\left(P_i^{-\theta}\right)\text{diag}\left(\Pi_i^{-\theta}\right)\text{diag}\left(p_i^{\theta}\right) - [\Xi_{ij}]\right)\text{diag}\left(Y_i^{-1}\right) \tag{A.22}$$

And inverting again:

$$[X_{ij}] = \text{diag}\left(Y_i\right)\left(\text{diag}\left(P_i^{-\theta}\right)\text{diag}\left(\Pi_i^{-\theta}\right)\text{diag}\left(p_i^{\theta}\right) - [\Xi_{ij}]\right)^{-1}\text{diag}\left(E_i\right) \tag{A.23}$$

The objective is now to express $\text{diag}\left(\Pi_i^{-\theta}\right)\text{diag}\left(p_i^{\theta}\right)$ as a function of observables only.

Starting from the definition $P_i^{-\theta} = \sum_j \tau_{ji}^{-\theta}\frac{Y_j}{\Pi_j^{-\theta}}$ and switching to matrix notations – where where $[x_i]$ denotes a $N \times 1$ column matrix of general term x_i:

$$\left[P_i^{-\theta}\right] = \left[\tau_{ij}^{-\theta}\right]'\left[\frac{Y_i}{\Pi_i^{-\theta}}\right] \tag{A.24}$$

$$\left[P_i^{-\theta}\right] = \left(\mathbf{I} - \mathbf{D}'\right)^{-1}\left[p_i^{-\theta}\frac{Y_i}{\Pi_i^{-\theta}}\right] \tag{A.25}$$

$$\left(\mathbf{I} - \text{diag}\left(p_i^{-\theta}\right)\text{diag}\left(\Pi_i^{\theta}\right)[\Xi_{ij}]'\,\text{diag}\left(P_i^{\theta}\right)\right)\left[P_i^{-\theta}\right] = \left[p_i^{-\theta}\frac{Y_i}{\Pi_i^{-\theta}}\right] \tag{A.26}$$

$$\left[\Pi_i^{-\theta}P_i^{-\theta}p_i^{\theta}\right] = [Y_i] + [\Xi_{ij}]'\,[1] \tag{A.27}$$

where $[1]$ is a $N \times 1$ column matrix in which all coefficients are equal to 1.

Similarly, starting from the definition $\Pi_i^{-\theta} = \sum_j \tau_{ij}^{-\theta}\frac{E_j}{P_j^{-\theta}}$ and switching to matrix notations:

$$\left[\Pi_i^{-\theta}\right] = \left[\tau_{ij}^{-\theta}\right]\left[\frac{E_i}{P_i^{-\theta}}\right] \tag{A.28}$$

$$\left[\Pi_i^{-\theta}\right] = (\mathbf{I} - \mathbf{G})^{-1} \left[p_i^{-\theta} \frac{E_i}{P_i^{-\theta}}\right] \tag{A.29}$$

with

$$\mathbf{G} = [g_{ij}] = \text{diag}\left(p_i^{-\theta}\right) \left[\tau_{ij}^{-\theta}\right]$$

$$\left(\mathbf{I} - \text{diag}\left(p_i^{-\theta}\right) \text{diag}\left(P_i^{\theta}\right) [\Xi_{ij}] \, \text{diag}\left(\Pi_i^{\theta}\right)\right) \left[\Pi_i^{-\theta}\right] = \left[p_i^{-\theta} \frac{E_i}{P_i^{-\theta}}\right] \tag{A.30}$$

$$\left[\Pi_i^{-\theta} P_i^{-\theta} p_i^{\theta}\right] = [E_i] + [\Xi_{ij}] \, [1] \tag{A.31}$$

where $[1]$ is a $N \times 1$ column matrix in which all coefficients are equal to 1.

Following A&A, I average the two definitions of $\text{diag}\left(\Pi_i^{-\theta}\right) \text{diag}\left(p_i^{\theta}\right)$:

$$\left[\Pi_i^{-\theta} P_i^{-\theta} p_i^{\theta}\right] = \frac{1}{2} [Y_i + E_i] + \frac{1}{2} \left([\Xi_{ij}]' \, [1] + [\Xi_{ij}] \, [1]\right) \tag{A.32}$$

Finally, plugging into the expression of $[X_{ij}]$ in equation A.23:

$$[X_{ij}] = \text{diag}\left(Y_i\right) \left(\text{diag}\left(\frac{1}{2} [Y_i + E_i] + \frac{1}{2} \left([\Xi_{ij}]' \, [1] + [\Xi_{ij}] \, [1]\right)\right) - [\Xi_{ij}]\right)^{-1} \text{diag}\left(E_i\right) \tag{A.33}$$

i.e., back to vectors notations:

$$X_{ij} = Y_i \left(\mathbf{D}^{\mathbf{X}} - [\Xi_{ij}]\right)^{-1}_{ij} E_j \tag{A.34}$$

where $\mathbf{D}^{\mathbf{X}} = \text{diag}\left(\frac{1}{2} [Y_i + E_i] + \frac{1}{2} \left([\Xi_{ij}]' \, [1] + [\Xi_{ij}] \, [1]\right)\right)$

A.5 Equilibrium with traffic

The first step consists in integrating the analytical relationship between τ_{ij} and t_{ij}, p_i into the equilibrium equations 12 and 13. Starting from the first equilibrium equation 12 and using expression A.7 yields:

$$\bar{A}_i^{-\theta} \bar{l}_i^{-\theta} y_i^{1+\theta} = \sum_j c_{ij}^G p_j^{-\theta} (1 + \kappa_j) y_j P_j^{\theta} \tag{A.35}$$

Switching to matrix notations:

$$\left[\bar{A}_i^{-\theta} \bar{l}_i^{-\theta} y_i^{1+\theta}\right] = \mathbf{C}^{\mathbf{G}} \left[p_i^{-\theta} (1 + \kappa_i) y_i P_i^{\theta}\right] \tag{A.36}$$

where $\left[\bar{A}_i^{-\theta} \bar{l}_i^{-\theta} y_i^{1+\theta}\right]$ and $\left[p_i^{-\theta} (1 + \kappa_i) y_i P_i^{\theta}\right]$ are $N \times 1$ column matrices and $\mathbf{C}^{\mathbf{G}}$ is a $N \times N$

square matrix. Remember that $\mathbf{C^G} = (\mathbf{I} - \mathbf{G})^{-1}$ from A.7, which yields:

$$(\mathbf{I} - \mathbf{G}) \left[\bar{A}_i^{-\theta} \bar{l}_i^{-\theta} y_i^{1+\theta} \right] = \left[p_i^{-\theta} (1 + \kappa_i) y_i P_i^{\theta} \right] \tag{A.37}$$

or in non-matrix notations:

$$\bar{A}_i^{-\theta} \bar{l}_i^{-\theta} y_i^{1+\theta} = p_i^{-\theta} (1 + \kappa_i) y_i P_i^{\theta} + \sum_j p_i^{-\theta} t_{ij}^{-\theta} \bar{A}_j \bar{l}_j^{-\theta} y_j^{\theta+1} \tag{A.38}$$

Similarly with the second equilibrium equation 13 and using expression A.8:

$$P_i^{-\theta} = \sum_j c_{ji}^{D} p_j^{-\theta} \bar{A}_j^{\theta} \bar{l}_j^{\theta} y_j^{-(\theta+1)} \tag{A.39}$$

Switching to matrix notations:

$$\left[P_i^{-\theta} \right] = \left[p_i^{-\theta} \bar{A}_i^{\theta} \bar{l}_i^{\theta} y_i^{-(\theta+1)} \right] \mathbf{C^{D'}} \tag{A.40}$$

where $\left[P_i^{-\theta} \right]$ and $\left[p_i^{-\theta} \bar{A}_i^{\theta} \bar{l}_i^{\theta} y_i^{-(\theta+1)} \right]$ are $N \times 1$ column matrices and $\mathbf{C^D}$ is a $N \times N$ square matrix. Remember that $\mathbf{C^D} = (\mathbf{I} - \mathbf{D})^{-1}$ from A.7, hence $\mathbf{C^{D'}} = (\mathbf{I} - \mathbf{D'})^{-1}$, which yields:

$$\left[P_i^{-\theta} \right] (\mathbf{I} - \mathbf{D'}) = \left[p_i^{-\theta} \bar{A}_i^{\theta} \bar{l}_i^{\theta} y_i^{-(\theta+1)} \right] \tag{A.41}$$

or in non-matrix notations:

$$P_i^{-\theta} = p_i^{-\theta} \bar{A}_i^{\theta} \bar{l}_i^{\theta} y_i^{-(\theta+1)} + \sum_j p_i^{-\theta} t_{ji}^{-\theta} P_j^{-\theta} \tag{A.42}$$

The second step consists in introducing the traffic congestion into equations A.38 and A.42. Combining equation 27 with expression A.1 yields

$$p_i = \bar{\Gamma}_i^{\frac{1}{1-\lambda\theta}} \, e^{\frac{\mu_i}{1-\lambda\theta} \text{ weather}_i} \, \bar{L}^{\frac{\lambda}{1-\lambda\theta}} \bar{A}_i^{\frac{-\lambda\theta}{1-\lambda\theta}} \bar{l}_i^{\frac{-\lambda\theta}{1-\lambda\theta}} P_i^{\frac{-\lambda\theta}{1-\lambda\theta}} \, y_i^{\frac{\lambda(\theta+1)}{1-\lambda\theta}} \tag{A.43}$$

Using this expression to replace p_i in equations A.38 and A.42 leads to the two equilibrium conditions with traffic:

$$\begin{aligned} y_i^{\theta+1+\frac{\lambda\theta(\theta+1)}{1-\lambda\theta}} P_i^{-\frac{\lambda\theta^2}{1-\lambda\theta}} =& \bar{L}^{-\frac{\lambda\theta}{1-\lambda\theta}} \bar{A}_i^{\frac{\lambda\theta^2}{1-\lambda\theta}+\theta} \bar{\Gamma}_i^{\frac{-\theta}{1-\lambda\theta}} e^{\frac{-\mu_i\theta}{1-\lambda\theta}\text{weather}_i} \bar{l}_i^{\frac{\lambda\theta^2}{1-\lambda\theta}+\theta} (1 + \kappa_i) y_i P_i^{\theta} \\ &+ \bar{L}^{-\frac{\lambda\theta}{1-\lambda\theta}} \sum_{j=1}^{N} \bar{A}_i^{\frac{\lambda\theta^2}{1-\lambda\theta}+\theta} \bar{A}_j \bar{t}_{ij}^{-\theta} \bar{\Gamma}_i^{\frac{-\theta}{1-\lambda\theta}} e^{\frac{-\mu_i\theta}{1-\lambda\theta}\text{weather}_i} \bar{l}_i^{\frac{\lambda\theta^2}{1-\lambda\theta}+\theta} \bar{l}_j^{-\theta} y_j^{1+\theta} \end{aligned} \tag{A.44}$$

$$y_i^{\frac{\lambda\theta(\theta+1)}{1-\lambda\theta}} P_i^{-\theta-\frac{\lambda\theta^2}{1-\lambda\theta}} = \bar{L}^{\frac{-\lambda\theta}{1-\lambda\theta}} \bar{A}_i^{\frac{\lambda\theta^2}{1-\lambda\theta}+\theta} \bar{\Gamma}_i^{\frac{-\theta}{1-\lambda\theta}} e^{\frac{-\mu_i\theta}{1-\lambda\theta}\text{weather}_i} \bar{l}_i^{\frac{\lambda\theta^2}{1-\lambda\theta}+\theta} y_i^{-\theta+1} + \bar{L}^{-\frac{\lambda\theta}{1-\lambda\theta}} \sum_{j=1}^{N} \bar{A}_i^{\frac{\lambda\theta^2}{1-\lambda\theta}} \bar{t}_{ij}^{-\theta} \bar{\Gamma}_i^{\frac{-\theta}{1-\lambda\theta}} e^{\frac{-\mu_i\theta}{1-\lambda\theta}\text{weather}_i} \bar{l}_i^{\frac{\lambda\theta^2}{1-\lambda\theta}} P_j^{-\theta} \tag{A.45}$$

A.6 Exact hat algebra

Consider a counterfactual weather $\{\text{weather}'_i\}_{i\in\mathcal{N}}$ and counterfactual trade deficits $\{(1+\kappa'_i)\}_{i\in\mathcal{N}}$. Combining the market clearing condition $Y_i = \sum_j X_{ij}$ from 8 with equation 9 yields

$$\Pi_i^{-\theta} = \sum_j \tau_{ij}^{-\theta} E_j P_j^{\theta} \tag{A.46}$$

Using equation A.8 and switching to matrix notations, it comes:

$$\left[\Pi_i^{-\theta}\right] = \left(\mathbf{I} - \left[p_i^{-\theta} t_{ij}^{-\theta}\right]\right)^{-1} \left[p_i^{-\theta} E_i P_i^{\theta}\right] \tag{A.47}$$

where $\left[\Pi_i^{-\theta}\right]$ and $\left[p_i^{-\theta} E_i P_i^{\theta}\right]$ are $N \times 1$ column matrices and $\left[p_i^{-\theta} t_{ij}^{-\theta}\right]$ is a $N \times N$ square matrix. This can be rewritten as

$$\Pi_i^{-\theta} = p_i^{-\theta} E_i P_i^{\theta} + \sum_j p_i^{-\theta} t_{ij}^{-\theta} \Pi_j^{-\theta} \tag{A.48}$$

Similarly, combining the market clearing condition $E_j = \sum_i X_{ij}$ from 8 with equation 9 yields

$$P_j^{-\theta} = \sum_j \tau_{ij}^{-\theta} Y_i \Pi_i^{\theta} \tag{A.49}$$

Using equation A.7 and switching to matrix notations, it comes:

$$\left[P_i^{-\theta}\right]' = \left[p_i^{-\theta} Y_i \Pi_i^{\theta}\right]' \left(\mathbf{I} - \left[p_j^{-\theta} t_{ij}^{-\theta}\right]\right)^{-1} \tag{A.50}$$

which can be rewritten as

$$P_j^{-\theta} = p_j^{-\theta} Y_j \Pi_j^{\theta} + \sum_i p_j^{-\theta} t_{ij}^{-\theta} P_i^{-\theta} \tag{A.51}$$

In the counterfactual scenario, equation A.48 will be:

$$\Pi_i'^{-\theta} = p_i'^{-\theta} E'_i P_i'^{\theta} + \sum_j p_i'^{-\theta} \bar{t}_{ij}^{-\theta} \Pi_j'^{-\theta} \tag{A.52}$$

where x' denote the counterfactual value of variable x. $\bar{t}_{ij}$ stays the same in the counterfactual world as it is exogenously given, hence not affected by a change in weather. Using the notation $\hat{x}_i \equiv \frac{x'_i}{x_i}$:

$$\hat{\Pi}_i'^{-\theta} = \frac{1}{\Pi_i^{-\theta}} p_i^{-\theta} E_i P_i^{\theta} \hat{p}_i^{-\theta} \hat{E}_i \hat{P}_i^{\theta} + \sum_j \frac{1}{\Pi_i^{-\theta}} p_i^{-\theta} \bar{t}_{ij}^{-\theta} \Pi_j^{-\theta} \hat{p}_i^{-\theta} \hat{\Pi}_j^{-\theta} \tag{A.53}$$

Using A.48 to replace $\Pi_i^{-\theta}$ and simplifying yields:

$$\hat{\Pi}_i'^{-\theta} = \frac{E_i}{E_i + \sum_j \bar{t}_{ij} P_i^{-\theta} \Pi_j^{-\theta}} \hat{p}_i^{-\theta} \hat{E}_i \hat{P}_i^{\theta} + \sum_j \left(\frac{\bar{t}_{ij} P_i^{-\theta} \Pi_j^{-\theta}}{E_i + \sum_j \bar{t}_{ij} P_i^{-\theta} \Pi_j^{-\theta}} \right) \hat{p}_i^{-\theta} \hat{\Pi}_j^{-\theta} \tag{A.54}$$

Remember that $\Xi_{ij} = \bar{t}_{ij} P_i^{-\theta} \Pi_j^{-\theta}$ (equation 20). Hence:

$$\hat{\Pi}_i^{-\theta} = \frac{E_i}{E_i + \sum_j \Xi_{ij}} \hat{p}_i^{-\theta} \hat{E}_i \hat{P}_i^{\theta} + \sum_j \left(\frac{\Xi_{ij}}{E_i + \sum_j \Xi_{ij}} \right) \hat{p}_i^{-\theta} \hat{\Pi}_j^{-\theta} \tag{A.55}$$

Similarly, equation A.51 will be in the counterfactual world:

$$P_j'^{-\theta} = p_j'^{-\theta} Y_j' \Pi_j'^{\theta} + \sum_i p_j'^{-\theta} \bar{t}_{ij}^{-\theta} P_i'^{-\theta} \tag{A.56}$$

which can be rewritten as:

$$\hat{P}_j^{-\theta} = \frac{1}{P_j^{-\theta}} \frac{p_j^{-\theta} Y_j}{\Pi_j^{-\theta}} \frac{\hat{p}_j^{-\theta} \hat{Y}_j}{\hat{\Pi}_j^{-\theta}} + \sum_i \frac{p_j^{-\theta} \bar{t}_{ij}^{-\theta} P_i^{-\theta}}{P_j^{-\theta}} \hat{p}_j^{-\theta} \hat{P}_i^{-\theta} \tag{A.57}$$

Using A.51 to replace $P_j^{-\theta}$ and the expression of Ξ_{ij} from equation 20 yields:

$$\hat{P}_j^{-\theta} = \frac{Y_j}{Y_j + \sum_i \Xi_{ij}} \frac{\hat{p}_j^{-\theta} \hat{Y}_j}{\hat{\Pi}_j^{-\theta}} + \sum_i \left(\frac{\Xi_{ij}}{Y_j + \sum_i \Xi_{ij}} \right) \hat{p}_j^{-\theta} \hat{P}_i^{-\theta} \tag{A.58}$$

From equation 27, we can write:

$$\hat{p}_i = e^{\frac{\mu_i}{1-\lambda\theta} \Delta \text{ weather}_i} \hat{P}_i^{\frac{-\lambda\theta}{1-\lambda\theta}} \hat{\Pi}_i^{\frac{-\lambda\theta}{1-\lambda\theta}} \tag{A.59}$$

Plugging this expression in equations A.55 and A.58 leads to:

$$\hat{\Pi}_i^{-\frac{\theta}{1-\lambda\theta}} \hat{P}_i^{-\frac{\theta}{1-\lambda\theta}} = \frac{E_i}{E_i + \sum_j \Xi_{ij}} \hat{E}_i \, e^{\frac{-\mu_i\theta}{1-\lambda\theta} \Delta \text{ weather}_i} + \sum_j \left(\frac{\Xi_{ij}}{E_i + \sum_j \Xi_{ij}} \right) e^{\frac{-\mu_i\theta}{1-\lambda\theta} \Delta \text{ weather}_i} \hat{P}_i^{-\theta} \hat{\Pi}_j^{-\theta} \tag{A.60}$$

$$\hat{P}_i^{-\frac{\theta}{1-\lambda\theta}} \hat{\Pi}_i^{-\frac{\theta}{1-\lambda\theta}} = \frac{Y_i}{Y_i + \sum_j \Xi_{ji}} \hat{Y}_i \, e^{\frac{-\mu_i\theta}{1-\lambda\theta} \Delta \text{ weather}_i} + \sum_j \left(\frac{\Xi_{ji}}{Y_i + \sum_j \Xi_{ji}} \right) e^{\frac{-\mu_i\theta}{1-\lambda\theta} \Delta \text{ weather}_i} \hat{P}_j^{-\theta} \hat{\Pi}_i^{-\theta} \tag{A.61}$$

Finally, from equation A.1 I get

$$\hat{\Pi}_i = \hat{y}_i^{-\frac{\theta+1}{\theta}} \tag{A.62}$$

and from equation 11 it comes

$$\hat{E}_i = \widehat{(1+\kappa_i)}\hat{y}_i \tag{A.63}$$

Plugging these two expressions into equations A.60 and A.61 yields the two exact hat equilibrium equations 30 and 31:

$$\begin{aligned}\hat{y}_i^{\frac{1+\theta}{1-\lambda\theta}}\hat{P}_i^{\frac{-\theta}{1-\lambda\theta}+\theta} = &\left(\frac{E_i}{E_i+\sum_j \Xi_{ij}}\right) e^{\frac{-\mu_i\theta}{1-\lambda\theta}\Delta\text{weather}_i}\widehat{(1+\kappa_i)}\hat{y}_i\hat{P}_i^{\theta} \\ &+\sum_{j=1}^{N}\left(\frac{\Xi_{ij}}{E_i+\sum_j \Xi_{ij}}\right) e^{\frac{-\mu_i\theta}{1-\lambda\theta}\Delta\text{weather}_i}\hat{y}_j^{\theta+1}\end{aligned} \tag{A.64}$$

$$\begin{aligned}\hat{y}_i^{\frac{\theta+1}{1-\lambda\theta}-(\theta+1)}\hat{P}_i^{\frac{-\theta}{1-\lambda\theta}} = &\left(\frac{Y_i}{Y_i+\sum_j \Xi_{ji}}\right) e^{\frac{-\mu_i\theta}{1-\lambda\theta}\Delta\text{weather}_i}\hat{y}_i^{-\theta} \\ &+\sum_{j=1}^{N}\left(\frac{\Xi_{ji}}{Y_i+\sum_j \Xi_{ji}}\right) e^{\frac{-\mu_i\theta}{1-\lambda\theta}\Delta\text{weather}_i}\hat{P}_j^{-\theta}\end{aligned} \tag{A.65}$$

B Data

Figure B.1: Correlation of the different weather variables

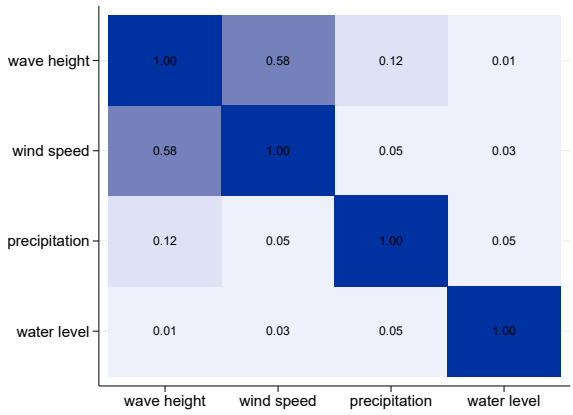
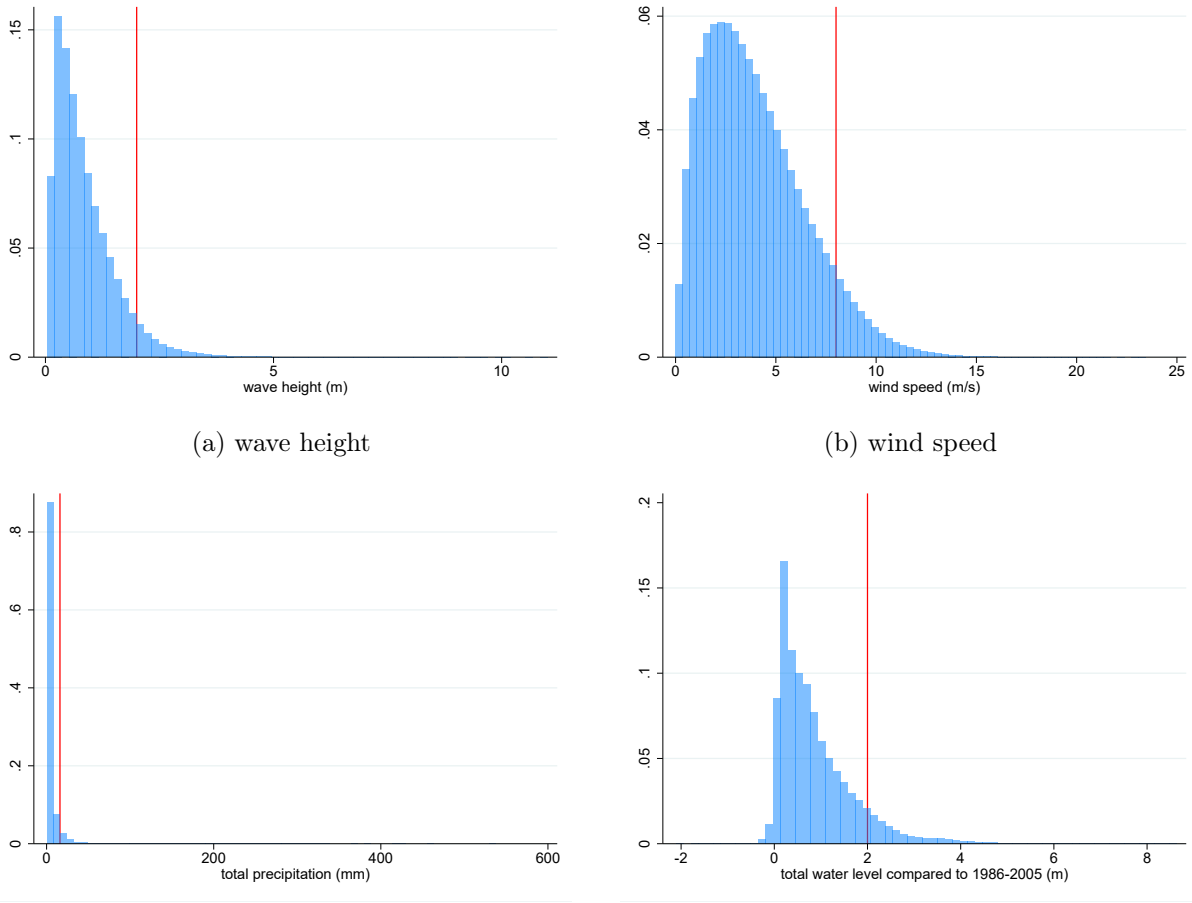


Figure B.2: Distribution of daily weather measures across ports



(a) wave height

(b) wind speed

(c) precipitation

(d) total water level

Note: The vertical red bars correspond to the absolute threshold values used in reduced-form exercises.

C Further reduced-form evidence

C.1 Other weather variables

Table C.1: Effect of wind speed on port efficiency (daily)

	(1) log time	(2) # calls	(3) log time	(4) # calls
wind speed	0.0041***	-0.0145***	0.0020***	-0.0144***
	(0.0005)	(0.0008)	(0.0006)	(0.0017)
date (day) FE	✓	✓		
port FE	✓	✓		
port-month FE			✓	✓
country-day FE			✓	✓
SE cluster level	port	port	country	country
# observations	2,024,358	5,223,035	1,818,063	4,134,985
# clusters	1,679	1,679	128	132

Standard errors in parentheses

* $p < 0.10$, ** $p < 0.05$, *** $p < 0.01$

Table C.2: Effect of wind speed higher than 8ms^{-1} on port efficiency (daily)

	(1) log time	(2) # calls	(3) log time	(4) # calls
wind speed $> 8\text{ms}^{-1}$	0.0266***	-0.1179***	0.0120***	-0.0907***
	(0.0041)	(0.0093)	(0.0040)	(0.0157)
date (day) FE	✓	✓		
port FE	✓	✓		
port-month FE			✓	✓
country-day FE			✓	✓
SE cluster level	port	port	country	country
# observations	2,024,358	5,223,035	1,818,063	4,134,985
# clusters	1,679	1,679	128	132

Standard errors in parentheses

* $p < 0.10$, ** $p < 0.05$, *** $p < 0.01$

Table C.3: Effect of wind speed higher than port 95th percentile on port efficiency (daily)

	(1) log time	(2) # calls	(3) log time	(4) # calls
wind speed > p95	0.0337***	-0.1536***	0.0222***	-0.1311***
	(0.0042)	(0.0083)	(0.0053)	(0.0246)
date (day) FE	✓	✓		
port FE	✓	✓		
port-month FE			✓	✓
country-day FE			✓	✓
SE cluster level	port	port	country	country
# observations	2,024,358	5,223,035	1,818,063	4,134,985
# clusters	1,679	1,679	128	132

Standard errors in parentheses

* $p < 0.10$, ** $p < 0.05$, *** $p < 0.01$

Table C.4: Effect of precipitation on port efficiency (daily)

	(1) log time	(2) # calls	(3) log time	(4) # calls
precipitation	0.0015***	-0.0027***	0.0009***	-0.0024***
	(0.0002)	(0.0002)	(0.0002)	(0.0004)
date (day) FE	✓	✓		
port FE	✓	✓		
port-month FE			✓	✓
country-year FE				
country-day FE			✓	✓
SE cluster level	port	port	country	country
# observations	1,291,266	3,418,675	1,151,276	2,625,652
# clusters	1,675	1,675	128	132

Standard errors in parentheses

* $p < 0.10$, ** $p < 0.05$, *** $p < 0.01$

Table C.5: Effect of precipitation higer than 16mm on port efficiency (daily)

	(1) log time	(2) # calls	(3) log time	(4) # calls
precipitation >16mm	0.0490***	-0.0642***	0.0302***	-0.0526***
	(0.0043)	(0.0047)	(0.0055)	(0.0092)
date (day) FE	✓	✓		
port FE	✓	✓		
port-month FE			✓	✓
country-day FE			✓	✓
SE cluster level	port	port	country	country
# observations	1,291,266	3,418,675	1,151,276	2,625,652
# clusters	1,675	1,675	128	132

Standard errors in parentheses

* $p < 0.10$, ** $p < 0.05$, *** $p < 0.01$

Table C.6: Effect of precipitation higher than port 95th percentile on port efficiency (daily)

	(1) log time	(2) # calls	(3) log time	(4) # calls
precipitation > p95	0.0490***	-0.0769***	0.0325***	-0.0612***
	(0.0041)	(0.0049)	(0.0054)	(0.0116)
date (day) FE	✓	✓		
port FE	✓	✓		
port-month FE			✓	✓
country-day FE			✓	✓
SE cluster level	port	port	country	country
# observations	1,291,266	3,418,675	1,151,276	2,625,652
# clusters	1,675	1,675	128	132

Standard errors in parentheses

* $p < 0.10$, ** $p < 0.05$, *** $p < 0.01$

C.2 Event-study setting

A weather shock might also have an effect before and after it is actually happening. To test this, I consider the effect of a binary treatment $\mathbb{1}\{\text{weather}_{it} > p99\text{weather}_i\}$ on the days before / after it happens, using an event study setting.[26] I rely on the local projection difference-in-differences (LP-DiD) setting of (Dube et al., 2023), to allow to non-absorbing treatment and potential multiple treatments:

$$y_{i,t+h} - y_{i,t-1} = \beta_h \Delta D_{it} + \delta_t^h + \delta_{im}^h + \epsilon_{it}^h \tag{C.66}$$

where D_{it} is the (binary) treatment status of port i on day t and Δ denotes first-difference operator, with sample restriction:

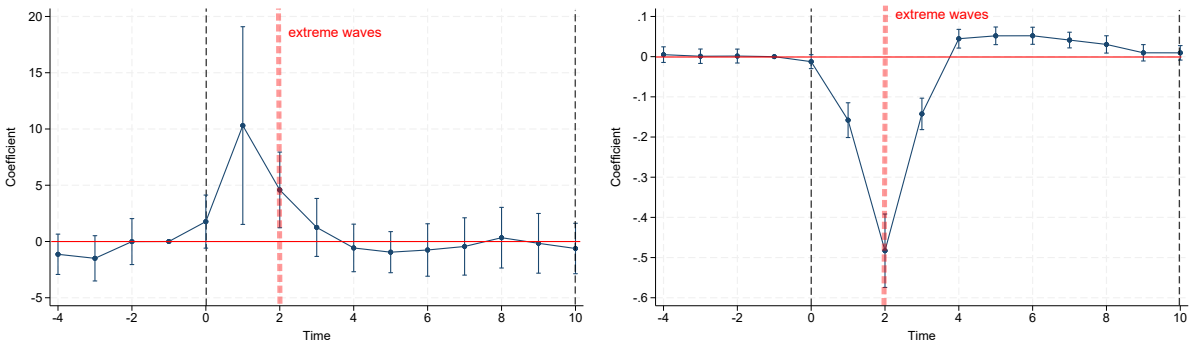
$$\begin{cases} \text{treatment:} & D_{i,t+j} = 1 \text{ for } 0 \leq j \leq h, \qquad D_{i,t-j} = 0 \text{ for } 1 \leq j \leq L \\ \text{clean control:} & D_{i,t-j} = 0 \text{ for } -h \leq j \leq L \end{cases} \tag{C.67}$$

where L is the number of periods after which the dynamic effects stabilize. I keep in the sample only clean treatment (ports that remain in treatment for the post-event window and that have not experienced a treatment close before the one we are considering) and clean controls (ports are not close to a treatment, either before or after). I also control for potential non-parallel trends with port-month fixed effects. To account for the fact that this setting assumes no anticipation and that the clean treated and control conditions assume no change of treatment status (i.e. no entry into treatment and no exit of treatment), I define treatment as 12 days around the extreme event (2 days before, 10 days after).

Figure C.3 show the results with weather measured as wave height. For dwell time, the effect is bigger one day before the event, but does not seem to last after. The number of port calls is reduced both before and after, but there seems to be a slight catch up afterwards – but which does not compensate the negative effect.

[26] With this definition of event, I am potentially comparing days where the wave height is above the 99th percentile, to days where it is slightly below: this would tend to attenuate the results.

Figure C.3: Event study results: effect extreme wave event on port efficiency



(a) Dwell time

(b) Number of entering calls

C.3 Reduced-form at the ship level

The data allow to estimate the effect of weather shocks on ships dwell time at the ship level (without aggregating to port daily averages):

$$\ln(\text{time}_{sit}) = \beta \text{ weather}_{it} + \delta_{si} + \delta_t + \delta_{iy} + \epsilon_{sit} \tag{C.68}$$

where s denotes a ship, i a port, t a day and y a year. time_{sit} is the dwell time experienced by ship s in port i on day t. weather_{it} is the weather at port i during day t – measured either by average daily wave height or by non-linear bins of wave height.

The results in the tables below show effects similar to the ones found at the port level: a worse weather (hight wave height, water level, wind speed, or precipitation) increases ship dwell time, an effect which is mostly driven by extreme events.

Table C.7: Effect of wave height on ship dwell time, at the ship level

log dwell time	(1)	(2)	(3)
wave height	0.0347***		
	(0.0021)		
wave height >2m		0.0604***	
		(0.0046)	
wave height >p95			0.0442***
			(0.0038)
date (day) FE	✓	✓	✓
ship-port FE	✓	✓	✓
port-year FE	✓	✓	✓
SE cluster level	ship, port	ship, port	ship, port
# observations	6,854,364	6,854,364	6,854,364
# clusters	1,676	1,676	1,676

Standard errors in parentheses

* $p < 0.10$, ** $p < 0.05$, *** $p < 0.01$

Table C.8: Effect of total water level on ship dwell time, at the ship level

log dwell time	(1)	(2)	(3)
water level	0.0203***		
	(0.0025)		
water level >2m		0.0068***	
		(0.0018)	
water level >p95			0.0213***
			(0.0023)
date (day) FE	✓	✓	✓
ship-port FE	✓	✓	✓
port-year FE	✓	✓	✓
SE cluster level	ship, port	ship, port	ship, port
# observations	6,875,918	6,875,918	6,875,918
# clusters	1,676	1,676	1,676

Standard errors in parentheses

* $p < 0.10$, ** $p < 0.05$, *** $p < 0.01$

Table C.9: Effect of wind speed on ship dwell time, at the ship level

	(1)	(2)	(3)
wind speed	0.0039***		
	(0.0005)		
wind speed >8ms^{-1}		0.0041***	
		(0.0012)	
wind speed >p95			0.0407***
			(0.0039)
date (day) FE	✓	✓	✓
ship-port FE	✓	✓	✓
port-year FE	✓	✓	✓
SE cluster level	ship, port	ship, port	ship, port
# observations	6,854,364	6,854,364	6,854,364
# clusters	1,676	1,676	1,676

Standard errors in parentheses

* $p < 0.10$, ** $p < 0.05$, *** $p < 0.01$

Table C.10: Effect of precipitation on ship dwell time, at the ship level

	(1)	(2)	(3)
precipitation	0.0012***		
	(0.0001)		
precipitation >16mm		0.0186***	
		(0.0015)	
precipitation >p95			0.0326***
			(0.0028)
date (day) FE	✓	✓	✓
ship-port FE	✓	✓	✓
port-year FE	✓	✓	✓
SE cluster level	ship, port	ship, port	ship, port
# observations	4,395,618	4,395,618	4,395,618
# clusters	1,662	1,662	1,662

Standard errors in parentheses

* $p < 0.10$, ** $p < 0.05$, *** $p < 0.01$

C.4 Effects outside of the port

When a port is disrupted, ships might prefer to wait outside of the port, to avoid paying additional port fees. This mechanism is not captured in the baseline specification as port calls data only allow to observe when ships actually enter inside the port. However, I can look at the effect of weather shocks in origin or departure port, on the duration of ships trips – i.e. the amount of time between the moment they leave their origin port and the moment they arrive at their destination port. If ships tend to wait outside of ports when there is bad weather, this should increase their trip time.

I consider the following specification:

$$log(\text{trip time})_{sod,t} = \beta_o \text{ weather}_{o,t} + \beta_d \text{ weather}_{d,t+\text{trip time}} + \delta_s + \delta_{od} + \delta_t + \epsilon_{sod,t} \quad \text{(C.69)}$$

where $\text{trip time}_{sod,t}$ is the trip time of ship s going from origin port o to destination port d on day t (day of departure), $\text{weather}_{o,t}$ is the weather in port of origin at the day of departure, $\text{weather}_{d,t+\text{trip time}}$ the weather in port of destination at the day of arrival. I consider different sets of fixed effects: day, route, ship, ship-route, route-year.

Table C.11 shows the results measuring weather as wave height. These results seem constant over the different sets of fixed effects. They confirm the hypothesized mechanism: +1m in wave height at the origin port increases trip duration by 1.3%, while +1m in wave height at the destination port increases trip duration by 2.2%. In column (4), I remove the shortest routes (trimming at the top and bottom 25%) to make sure that the weather along the route is not correlated with weather in the ports of departure and arrival, and still find a positive and significant effect.

This means the effects measured *inside* the ports might be only a lower bound of the full effects, since they do not capture ships waiting *outside* of ports.

Table C.11: Effect of origin and destination ports wave height on ships trip duration

	(1)	(2)	(3)	(4)
wave height at origin port	0.0139***	0.0133***	0.0135***	0.0159***
	(0.0011)	(0.0012)	(0.0012)	(0.0015)
wave height at destination port	0.0222***	0.0224***	0.0224***	0.0279***
	(0.0011)	(0.0012)	(0.0012)	(0.0016)
date (day) FE	✓	✓	✓	✓
route (o-d) FE	✓			
ship FE	✓			
ship-route FE		✓	✓	✓
route-year FE			✓	✓
route distance restriction				✓
# observations	5,770,534	5,289,930	5,278,881	2,652,050
# routes	14,109	14,101	14,054	7,137

Standard errors in parentheses

* $p < 0.10$, ** $p < 0.05$, *** $p < 0.01$

C.5 Routes vs Ports

Delays in shipping can also happen because of weather conditions along the maritime route, i.e. in the journey between two ports. I compare the effects on shipping of weather along the maritime route and weather in the port, using the following specification:

$$\text{time}_{sit} = \beta \text{ weather}_{it} + \delta_{si} + \delta_t + \delta_{im} + \delta_{iy} + \epsilon_{sit} \tag{C.70}$$

where s is a ship, i either a *route* or a *port*, and t a day. time_{sit} denotes the time (in hours) spent by ship s along the route i or in the port i[27], $weather_{it}$ denotes the weather conditions (wave height) along the route i or in the port i – measured either as average daily wave height or bins of daily wave height. I also include ship-port (resp. ship-route) fixed effects, date fixed effects, port-month-of-the-year (resp. route-month-of-the-year) fixed effects, and port-year (resp. route-year) fixed effects.

To measure shipping time and weather along the maritime routes, I focus on trips happening on the 300 most frequent routes present in the shipping data. I compute trip duration as the difference between the time of destination port arrival and origin port departure. Since I only observe the origin and destination ports and not the exact trajectory of the ship in between, I rely on SeaRoute algorithm to compute the shortest route by sea between these two ports. Using gridded wave height from ERA5, I compute the weather along a route for a given day

[27] To ensure a better comparability between ports and routes, the dependent variable is in levels rather than in log, to quantify the effect in terms of additional hours of shipping.

as a weighted average of the grid points weather, where the weights are the inverse of distance between the grid point and the route, times a measure of the density of grid cells at the point location.

The results in Table C.12 show that the effect on weather along the route or in the port tend to be pretty similar: an increase of 1m of average wave height along the route or at the port increases shipping time by 0.7 hour. Port extreme weather events seems to have a slightly more important effect than route extreme weather events: a wave height greater than 2m at the port adds 1.5 hour of shipping time compared to a wave height lower than 0.5m, again 1.2 additional hour for a wave height greater than 2m at along the route.

Table C.12: Direct effect of weather on shipping time – comparison between routes and ports

	route weather on route time		port weather on port time	
	(1)	(2)	(3)	(4)
average wave	0.6791***		0.6795***	
	(0.0773)		(0.1198)	
wave <0.5m		*ref*		*ref*
wave 0.5-0.8m		0.0597		0.0894
		(0.0419)		(0.1000)
wave 0.8-1.3m		0.1472**		0.3137**
		(0.0601)		(0.1432)
wave 1.3-2m		0.4616***		0.5767***
		(0.0986)		(0.2009)
wave >2m		1.2374***		1.4580***
		(0.1480)		(0.2454)
unit	route	route	port	port
date (day) FE	✓	✓	✓	✓
ship-unit FE	✓	✓	✓	✓
unit-month FE	✓	✓	✓	✓
unit-year FE	✓	✓	✓	✓
# observations	1,555,030	1,555,030	6,905,453	6,905,453
# clusters	255	255	1,664	1,664

Standard errors in parentheses

* $p < 0.10$, ** $p < 0.05$, *** $p < 0.01$

Weather at port hence seems to be only marginally more important than weather at sea. However, weather at port can influence time spent on the route, as highlighted in section C.4,

because ships tend to lower their speed (or stop) when their destination port is congested. But weather along the route seems more unlikely to influence the time spent at ports. To test these mechanisms, I consider a similar specification:

$$\text{time}_{sit} = \beta \text{ weather}_{jt} + \delta_{si} + \delta_t + \delta_{im} + \delta_{iy} + \epsilon_{sit} \tag{C.71}$$

where either i is a route, in which case j is the destination port of this route – i.e. I measure the effect of weather in the destination port on the time spend on the route (expected to be positive, as in section C.4); or i is a port, in which case j is a route arriving at port i – i.e. I investigate the effect of weather along a route on the time spent in destination port (expected to be close to null).

Table C.13: Cross effect of weather on shipping time – comparison between routes and ports

	port weather on route time		route weather on port time	
	(1)	(2)	(3)	(4)
average wave	0.9510***		0.0863	
	(0.0489)		(0.0794)	
wave <0.5m		*ref*		*ref*
wave 0.5-0.8m		0.2030***		-0.2766**
		(0.0314)		(0.1207)
wave 0.8-1.3m		0.5284***		-0.2444*
		(0.0421)		(0.1457)
wave 1.3-2m		1.0529***		-0.1409
		(0.0636)		(0.1543)
wave >2m		1.8893***		0.2233
		(0.1136)		(0.2036)
weather unit	port route	port route	route port	route port
date (day) FE	✓	✓	✓	✓
ship-unit FE	✓	✓	✓	✓
unit-month FE	✓	✓	✓	✓
unit-year FE	✓	✓	✓	✓
# observations	5,265,994	5,265,994	426,331	426,331
# clusters	13,605	13,605	101	101

Standard errors in parentheses

* $p < 0.10$, ** $p < 0.05$, *** $p < 0.01$

The results in Table C.13 show that indeed, port weather can have a significant effect on time spent along the route (columns 1 and 2), but the reverse is not true (columns 3 and 4). Hence

adverse weather conditions in a port increase significantly the shipping time, both because of higher time spent in the port and along the route ; while time at sea has a smaller effect, only along the route. This justifies focusing on the effects of weather in the ports.

C.6 Alternative specifications for spillovers

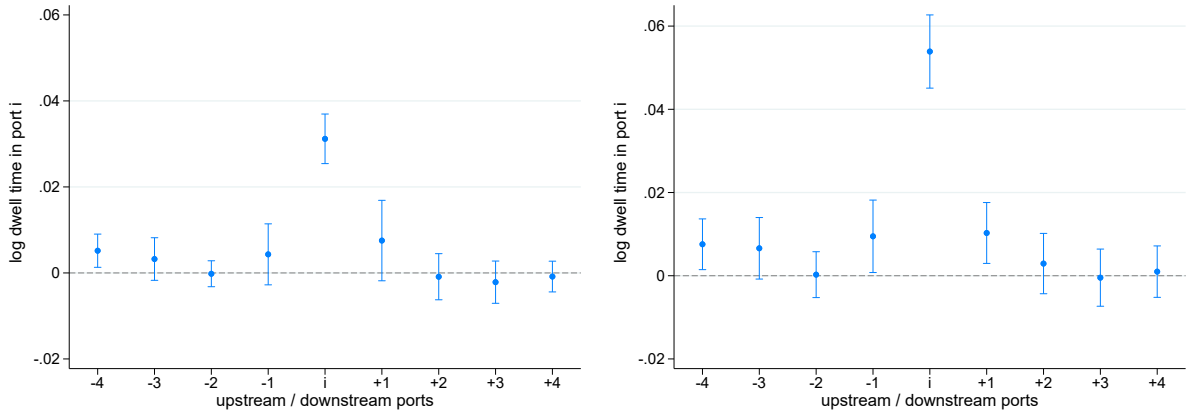
Instead of considering weather shocks in upstream ports $i-h$ and downstream ports $i+h$ on the *same day* t as the the ship s arrives in port i, as in the main specification 2, one might consider alternative specifications with leads and lags.

The first alternative specification accounts for the weather in different up and down-stream ports on the day day ship s visited them:

$$\ln(\text{time}_{sit}) = \sum_{h=0}^{4} \beta_h^U \text{ wave}_{i-h,t_{-h}} + \beta \text{ wave}_{i,t} + \sum_{h=0}^{4} \beta_h^D \text{ wave}_{i+h,t_{+h}} + \delta_{si} + \delta_t + \delta_{iy} + \epsilon_{sit} \quad \text{(C.72)}$$

where t_{-h} is the day at which the ship s stopped at the port $i-h$ (so *before* t), and t_{+h} is the day at which the ship s stopped at the port $i+h$ (so *after* t).

Figure C.4: Effect of upstream, local, and downstream wave height on port efficiency - with exact leads and lags



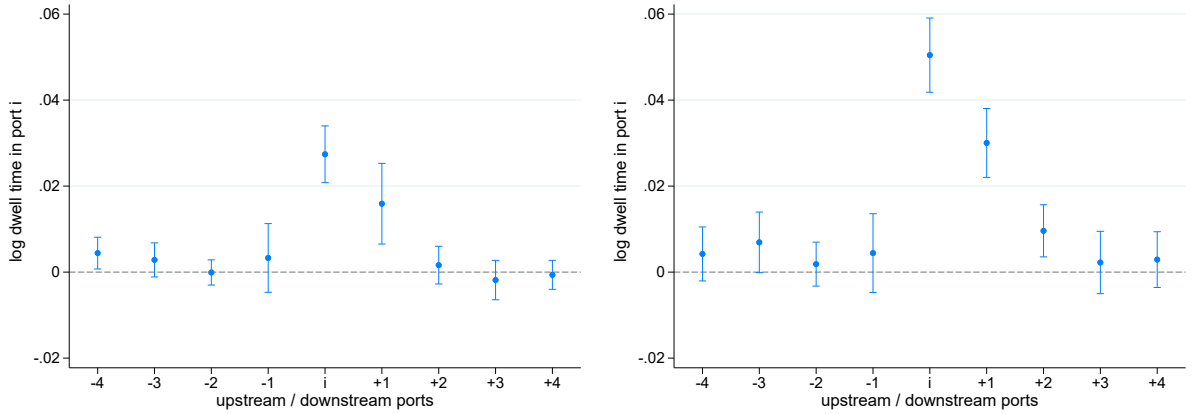
(a) average wave height

(b) wave height >2m

As the exact day at which the ship s visited the different ports might be endogenous on weather shocks in these ports, the second alternative specification arbitrarily considers exactly 1 day of delay between successive ports:

$$\ln(\text{time}_{sit}) = \sum_{h=0}^{4} \beta_h^U \text{ wave}_{i-h,t-h} + \beta \text{ wave}_{i,t} + \sum_{h=0}^{4} \beta_h^D \text{ wave}_{i+h,t+h} + \delta_{si} + \delta_t + \delta_{iy} + \epsilon_{sit} \quad \text{(C.73)}$$

Figure C.5: Effect of upstream, local, and downstream wave height on port efficiency – with arbitrary leads and lags



(a) average wave height

(b) wave height >2m

D Additional estimation results

Table D.14: Effect of moving average traffic and extreme waves (2m) and total water level on port dwell time

	(1)	(2) OLS	(3) IV
share days >2m (MA)	0.08178***	0.07645***	0.07222***
	(0.01046)	(0.00927)	(0.00875)
water level (MA)	0.02167***	0.01251*	0.00524
	(0.00661)	(0.00651)	(0.00695)
log traffic (MA)		0.13731***	0.24620***
		(0.00636)	(0.03514)
date FE	✓	✓	✓
ship-port FE	✓	✓	✓
port-year FE	✓	✓	✓
# observations	6,114,910	6,114,910	6,114,910
# ships	11,311	11,311	11,311
# ports	1,620	1,620	1,620
First Stage KP-F			155.4

Standard errors in parentheses

* $p < 0.10$, ** $p < 0.05$, *** $p < 0.01$

Table D.15: Effect of moving average traffic and wave extreme height (2m) and water level on port dwell time with adaptation

	(1)	(2)	(3)
share days >2m (MA)	0.12250***	0.11558***	0.11012***
	(0.01432)	(0.01255)	(0.01226)
share days >2m (MA) × period-avg	-0.23828***	-0.22910***	-0.22184***
	(0.06405)	(0.05948)	(0.05867)
water level (MA)	0.03029***	0.01757*	0.00751
	(0.00998)	(0.00949)	(0.00943)
waterlevel (MA) × period-avg	-0.00702**	-0.00477	-0.00300
	(0.00354)	(0.00346)	(0.00364)
log traffic (MA)		0.13727***	0.24581***
		(0.00636)	(0.03521)
date FE	✓	✓	✓
ship-port FE	✓	✓	✓
port-year FE	✓	checkmark	✓
# observations	6,114,910	6,114,910	6,114,910
# ships	11,311	11,311	11,311
# ports	1,620	1,620	1,620
First Stage KP-F			155.3

Standard errors in parentheses

* $p < 0.10$, ** $p < 0.05$, *** $p < 0.01$

E Computing counterfactuals

The international trade setting requires to take into account trade deficit between locations. I follow the trade literature to handle this feature in the empirical application, in two steps.

First, given baseline $\{\Xi_{ij0}, Y_{i0}, E_{i0}\}$ observed in the data, I compute counterfactual outcomes assuming no weather shock ($\Delta\text{weather}_i = 0 \quad \forall i \in \mathcal{N}$), but deficits go to zero ($\kappa_i' = 0$, i.e. $\widehat{(1+\kappa_i)} = \frac{1}{1+\kappa_i} = \frac{Y_i}{E_i} \quad \forall i \in \mathcal{N}$). It amounts to solving the following system of equations:

$$\hat{y}_{i1}^{\frac{1+\theta}{1-\lambda\theta}} \hat{P}_{i1}^{\frac{-\theta}{1-\lambda\theta}+\theta} = \left(\frac{Y_{i0}}{E_{i0} + \sum_j \Xi_{ij0}}\right) \hat{y}_{i1} \hat{P}_{i1}^{\theta} + \sum_{j=1}^{N} \left(\frac{\Xi_{ij0}}{E_{i0} + \sum_j \Xi_{ij0}}\right) \hat{y}_{j1}^{\theta+1} \tag{E.74}$$

$$\hat{y}_{i1}^{\frac{\theta+1}{1-\lambda\theta}-(\theta+1)} \hat{P}_{i1}^{\frac{-\theta}{1-\lambda\theta}} = \left(\frac{Y_{i0}}{Y_{i0} + \sum_j \Xi_{ji0}}\right) \hat{y}_{i1}^{-\theta} + \sum_{j=1}^{N} \left(\frac{\Xi_{ji0}}{Y_{i0} + \sum_j \Xi_{ji0}}\right) \hat{P}_{j1}^{-\theta} \tag{E.75}$$

This allows to retrieve first step counterfactual levels of outcome $Y_{i1} = Y_{i0}\ \hat{y}_{i1}$ and traffic flows $\Xi_{ij1} = \Xi_{ij0}\ \hat{\Xi}_{ij1}$: those are the outcome levels if the weather profile stays the same as in the baseline period, but the trade gets balanced. By definition, we then have $Y_{i1} = E_{i1}$.

Second, given $\{\Xi_{ij1}, Y_{i1}\}$ resulted form the first step, I compute counterfactual outcomes assuming that the trade deficits stay to zero ($\kappa_i = \kappa_i' = 0$, $\widehat{(1+\kappa_i)} = 1 \quad \forall i \in \mathcal{N}$) but that weather changes ($\{\Delta\text{weather}_i\}_{i\in\mathcal{N}}$). It amounts to solving the following system of equations:

$$\hat{y}_{i2}^{\frac{1+\theta}{1-\lambda\theta}} \hat{P}_{i2}^{\frac{-\theta}{1-\lambda\theta}+\theta} = \left(\frac{Y_{i1}}{E_{i1} + \sum_j \Xi_{ij1}}\right) e^{\frac{-\mu_i\theta}{1-\lambda\theta}\Delta\text{weather}_i} \hat{y}_{i2} \hat{P}_{i2}^{\theta} + \sum_{j=1}^{N} \left(\frac{\Xi_{ij1}}{Y_{i1} + \sum_j \Xi_{ij1}}\right) e^{\frac{-\mu_i\theta}{1-\lambda\theta}\Delta\text{weather}_i} \hat{y}_{j2}^{\theta+1} \tag{E.76}$$

$$\hat{y}_{i2}^{\frac{\theta+1}{1-\lambda\theta}-(\theta+1)} \hat{P}_{i2}^{\frac{-\theta}{1-\lambda\theta}} = \left(\frac{Y_{i1}}{Y_{i1} + \sum_j \Xi_{ji1}}\right) e^{\frac{-\mu_i\theta}{1-\lambda\theta}\Delta\text{weather}_i} \hat{y}_{i2}^{-\theta} + \sum_{j=1}^{N} \left(\frac{\Xi_{ji1}}{Y_{i1} + \sum_j \Xi_{ji1}}\right) e^{\frac{-\mu_i\theta}{1-\lambda\theta}\Delta\text{weather}_i} \hat{P}_{j2}^{-\theta} \tag{E.77}$$

I compute the treatment effect of the change in weather as the difference between equilibrium levels in the two counterfactuals, i.e. nominal outcome changes $\hat{y}_{i2}$ and real outcome changes $\hat{y}_{i2}/\hat{P}_{i2}$.

This method is standard in international trade literature to address deficits (Ossa, 2016). An alternative approach would be to compute just one counterfactual holding the deficits fixed relative to the observed equilibrium; however, this method causes convergence issues.

F Algorithm for conducting counterfactuals

I adapt the algorithm of Allen & Arkolakis (2022) to find the equilibrium in our counterfactual simulations. It consists of a loop solving for vectors of $\{\hat{y}_i\}$ and $\{\hat{P}_i\}$. Equilibrium equations 30 and 31 form a system of non-linear equations in $\{\hat{y}_i\}$ and $\{\hat{P}_i\}$. At the same time, the term on the left-hand side of each of the equilibrium conditions is a log-linear combination of the endogenous variables.

I start with an initial guess of the endogenous variables $\{\hat{y}_i\}_{(0)} = 1$ and $\{\hat{P}_i\}_{(0)} = 1$ and plug it into the equilibrium conditions 30 and 31. To help us update the guess, I define the following:

$$\hat{x}_{1,i} \equiv \hat{y}_i^{\theta+1+\frac{\lambda\theta(\theta+1)}{1-\lambda\theta}} \hat{P}_i^{-\frac{\lambda\theta^2}{1-\lambda\theta}}$$

$$\hat{x}_{2,i} \equiv \hat{y}_i^{\frac{\lambda\theta(\theta+1)}{1-\lambda\theta}} \hat{P}_i^{-\theta-\frac{\lambda\theta^2}{1-\lambda\theta}}$$

so that:

$$\begin{pmatrix} \ln \hat{x}_{1,i} \\ \ln \hat{x}_{2,i} \end{pmatrix} = \begin{pmatrix} \theta+1+\frac{\lambda\theta(\theta+1)}{1-\lambda\theta} & -\frac{\lambda\theta^2}{1-\lambda\theta} \\ \frac{\lambda\theta(\theta+1)}{1-\lambda\theta} & -\theta-\frac{\lambda\theta^2}{1-\lambda\theta} \end{pmatrix} \begin{pmatrix} \ln \hat{y}_i \\ \ln \hat{P}_i \end{pmatrix} \iff$$

$$\begin{pmatrix} \ln \hat{y}_i \\ \ln \hat{P}_i \end{pmatrix} = \begin{pmatrix} \theta+1+\frac{\lambda\theta(\theta+1)}{1-\lambda\theta} & -\frac{\lambda\theta^2}{1-\lambda\theta} \\ \frac{\lambda\theta(\theta+1)}{1-\lambda\theta} & -\theta-\frac{\lambda\theta^2}{1-\lambda\theta} \end{pmatrix}^{-1} \begin{pmatrix} \ln \hat{x}_{1,i} \\ \ln \hat{x}_{2,i} \end{pmatrix}$$

By this definition, for a guess of $\left(\{\hat{y}_i\}_{(0)}, \{\hat{P}_i\}_{(0)}\right)$, the equilibrium conditions yield a set of vectors $\left(\{\hat{x}_{1,i}\}_{(1)}, \{\hat{x}_{2,i}\}_{(1)}\right)$, which by the log-linear transformation defined above, imply an updated guess of $\left(\{\hat{y}_i\}_{(1)}, \{\hat{P}_i\}_{(1)}\right)$. On each iteration, I rescale the vectors $\left(\{\hat{x}_{1,i}\}_{(1)}, \{\hat{x}_{2,i}\}_{(1)}\right)$ such that the second period income distribution still sums to 1, and update the guess of $\left(\{\hat{y}_i\}_{(0)}, \{\hat{P}_i\}_{(0)}\right)$ towards $\left(\{\hat{x}_{1,i}\}_{(1)}, \{\hat{x}_{2,i}\}_{(1)}\right)$. I iterate through this procedure until the equilibrium conditions are solved. Therefore, this loop returns a $\left(\{\hat{y}_i\}_{(0)}, \{\hat{P}_i\}_{(0)}\right)$ for which:[28]

$$(\hat{x}_{1,i})_{(1)} = \left(\frac{E_i}{E_i + \sum_j \Xi_{ij}}\right) e^{\frac{-\mu_i\theta}{1-\lambda\theta}\Delta\text{weather}_i} (\hat{y}_i)_{(0)} (\hat{P}_i)_{(0)}^{\theta} + \sum_{j=1}^{N} \left(\frac{\Xi_{ij}}{E_i + \sum_j \Xi_{ij}}\right) e^{\frac{-\mu_i\theta}{1-\lambda\theta}\Delta\text{weather}_i} (\hat{y}_j)_{(0)}^{\theta+1}$$

[28] This system assumes a constant deficit ratio κ; however the system can be adapted straightforwardly to consider rather a change in trade deficit, as done in the first step of Section E.

$$(\hat{x}_{2,i})_{(1)} = \left(\frac{Y_i}{Y_i + \sum_j \Xi_{ji}}\right) e^{\frac{-\mu_i \theta}{1-\lambda\theta}\Delta\text{weather}_i} (\hat{y}_i)_{(0)}^{-\theta} + \sum_{j=1}^{N} \left(\frac{\Xi_{ji}}{Y_i + \sum_j \Xi_{ji}}\right) e^{\frac{-\mu_i \theta}{1-\lambda\theta}\Delta\text{weather}_i} (\hat{P}_j)_{(0)}^{-\theta}$$

G Additional counterfactual results

Figure G.6: Changes in water level at the port level under scenario SSP5-8.5

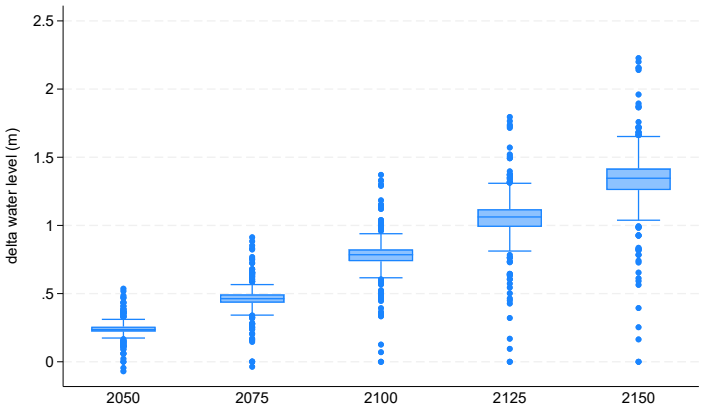
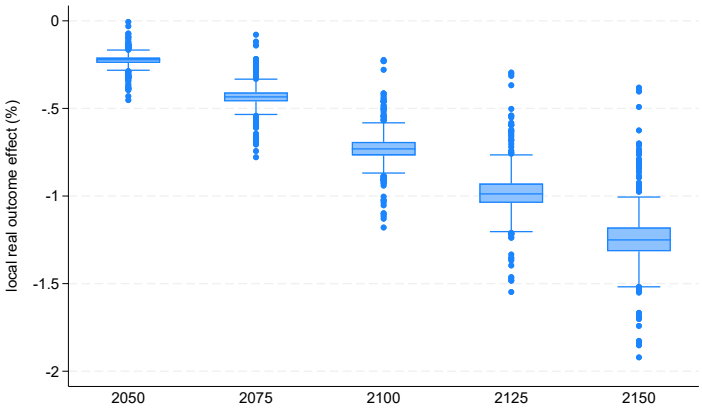
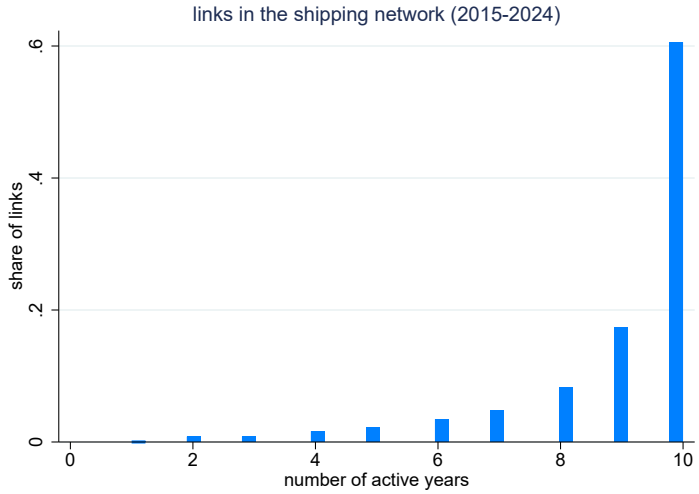


Figure G.7: Changes in real outcome at the port level under scenario SSP5-8.5



H Additional elements towards a flexible network

Figure H.8: Activity duration of links observed in the shipping data



Effect of weather on the number of links in a port I want to investigate if the weather conditions of a port might affect the network structure around this port – i.e. the number of active links serving this port. To do so, I consider the following specification:

$$n_{it} = \beta \text{ weather}_{i,[t-X,t]} + \delta_{iy} + \delta_t + \epsilon_{it} \tag{H.78}$$

where n_{it} is either the number of links arriving in port i during month t, or the number of links leaving from this port, or the number of active links (= arriving or leaving). I consider weather in the port over the past six months, measured as the share of days where wave height is greater than 2m. Table H.16 shows significant but small effects: switching from 0% to 100% of days with extreme wave height in the past 6 months in a port, reduces the number of active links (avg = 18) by 1 to 2%.

Table H.16: Effect of moving average wave height on the number of active links in a port

	ppml			log		
	(1)	(2)	(3)	(4)	(5)	(6)
	# arriving	# leaving	# active	# arriving	# leaving	# active
share days > 2m (MA)	-0.00734***	-0.00885***	-0.00809***	-0.01768***	-0.01459***	-0.02124***
	(0.00276)	(0.00270)	(0.00240)	(0.00417)	(0.00420)	(0.00405)
# observations	128,202	127,101	131,572	126,617	125,568	129,987

Standard errors in parentheses

* $p < 0.10$, ** $p < 0.05$, *** $p < 0.01$